PREGNANCY ASSOCIATED PLASMA PROTEIN-A2 (PAPP-A2) CONTRIBUTES TO THE REGULATION OF SKELETAL GROWTH IN MICE

by

Neilab Amiri

B.Sc., Simon Fraser University, 2011

Thesis Submitted in Partial Fulfillment of the
Requirements for the Degree of
Master of Science

in the
Department of Biological Sciences
Faculty of Science

SIMON FRASER UNIVERSITY

Spring 2015

Approval

Name:	**Neilab Amiri**
Degree:	**Master of Science**
Title:	***Pregnancy Associated Plasma Protein-A2 (PAPP-A2) contributes to the regulation of skeletal growth in mice***
Examining Committee:	**Chair:** Dr. Sherryl Bisgrove Associate Professor

Dr. Julian Christians
Senior Supervisor
Associate Professor _____

Dr. Gordon Rintoul
Supervisor
Associate Professor _____

Dr. Robert Young
Supervisor
Professor
Department of Chemistry _____

Dr. Tony Williams
Internal Examiner
Professor _____

Date Defended/Approved: March 17, 2015

Partial Copyright Licence

Ethics Statement

The author, whose name appears on the title page of this work, has obtained, for the research described in this work, either:

a. human research ethics approval from the Simon Fraser University Office of Research Ethics,

or

b. advance approval of the animal care protocol from the University Animal Care Committee of Simon Fraser University;

or has conducted the research

c. as a co-investigator, collaborator or research assistant in a research project approved in advance,

or

d. as a member of a course approved in advance for minimal risk human research, by the Office of Research Ethics.

A copy of the approval letter has been filed at the Theses Office of the University Library at the time of submission of this thesis or project.

The original application for approval and letter of approval are filed with the relevant offices. Inquiries may be directed to those authorities.

Simon Fraser University Library
Burnaby, British Columbia, Canada

update Spring 2010

Abstract

Pregnancy associated plasma protein-A2 (PAPP-A2) is a metalloproteinase that cleaves insulin like growth factor binding protein-5 (IGFBP-5), the most abundant IGFBP in bone. Deletion of the *Pappa2* gene reduces post-natal growth and skeletal size in mice. This research aimed to further understand the role of PAPP-A2 in skeletal physiology using mice with *Pappa2* disrupted constitutively, spatially (in bone), or temporally (in adulthood). I demonstrate that PAPP-A2 produced in bone AND other tissues regulates post-natal growth and skeletal size. Constitutive *Pappa2* deletion increases cortical bone mineral density (BMD), whereas disruption of *Pappa2* in adulthood decreases trabecular BMD in males alone. PAPP-A2, therefore, appears to play age-specific and potentially site-specific roles. Currently, there is a need for anabolic agents for the treatment of diseases like osteoporosis, making PAPP-A2 an interesting avenue of research.

Keywords: PAPP-A2, IGFBP-5, Bone, IGF, BMD, Osteoporosis

Acknowledgements

I would like to thank my senior supervisor, Dr. Julian Christians, for his mentorship and my committee members, Dr. Gordon Rintoul and Dr. Robert Young, for their time and input.

Thank you to Diana Duan, Katrina Juwono and James Topham for assisting with dissections, bone measurements and genotyping. I also thank the Animal Care staff at Simon Fraser University for assistance with animal maintenance and blood sampling. Additionally, I am indebted to Dr. Boa Ping Song and the histology department at the Child and Family Research Institute for their services. I would like to extend my appreciations to John Schipilow at the UBC Centre for High-Throughput Phenogenomics for his constant guidance and help with the analysis of my samples for Chapter 3.

Many thanks to my colleagues, Dr. Eunice Chin, Dr. Allison Cornell, and former colleague, Erin Crosely, for their guidance and friendship over the years. On a personal note, I would like to thank my parents and my sisters for their love and support throughout my life. To my best friend, Alf, thank you for keeping me motivated and mentally replenished. Lastly, I want to thank Dr. Sherryl Bisgrove and my uncle Dr. Ahmad Sidiqui for encouraging and inspiring me to pursue a career in Biology.

Table of Contents

List of Tables

List of Figures

Chapter 1.

Introduction

1.1. The skeleton and osteoporosis

The skeleton not only aids in structural support and mobility, but also serves to protect soft tissues, promote hematopoiesis, maintain mineral balance, and contain reserves of cell signalling peptides (Clarke, 2008). All bones are comprised of cortical (compact) and trabecular (spongy/cancellous) bone (Clarke, 2008). Both cortical and trabecular bone accumulate layer upon layer as collagen fibrils are deposited in a disorganized pattern and later mineralized, giving the bone its rigid nature and ultimately strengthening it (Clarke, 2008). Collagen is a major component of bone matrix and is deposited by bone forming cells prior to mineralization (Viguet-Carrin et al., 2006). The two major types of cells present in bone include osteoblasts and osteoclasts (Clarke, 2008). Osteoblasts (bone-forming cells) synthesize and secrete bone matrix and can differentiate into other bone cells to further regulate and maintain mineralisation (Kular et al., 2012). In contrast, osteoclasts are bone-resorptive cells that work in conjunction with osteoblasts to maintain, repair, and remodel bones (Kular et al., 2012). Together, the balance of osteoblast and osteoclast activity determines amount of bone present and consequently bone strength and health (Clarke, 2008; Kular et al., 2012).

Osteoporosis is a skeletal disorder that involves loss of bone mass and alterations of bone microarchitecture (Rizzoli et al., 2001). Each year, over 8 million bone fractures are attributed to osteoporosis globally (Johnell and Kanis, 2006) and with an aging population, the prevalence of osteoporotic fractures is predicted to increase by 200-300% over the next 40 years (Gullberg et al., 1997). The increasing occurrence of osteoporosis emphasizes a need for better preventative and therapeutic measures. Clinically, osteoporosis can be divided into two sub-types depending on the gender, age, and health of the patient: postmenopausal (Type I) osteoporosis is more common amongst women

after menopause, while senile (Type II) osteoporosis can occur in both sexes after the age of 70 (Shen et al., 2003). Type I osteoporosis is characterized by the loss of trabecular bone and is mainly due to estrogen deficiency, whereas both cortical and trabecular parameters are affected in Type II osteoporosis (Shen et al., 2003)

At any adult age, skeletal integrity is determined by the balance between the amount of bone accumulated during growth and age-related bone loss (Rizzoli et al., 2001). Peak bone mineral density is the maximum bone mass achieved during puberty, and differs between the sexes, with males reaching higher levels by the end of growth (Bonjour et al., 2009; Heaney et al., 2000). However, the rate of bone turnover between cortical and trabecular bone can differ greatly such that trabecular bone has a higher rate of remodelling (is more actively broken down and replaced by new bone) (Alma Y. et al., 2013; Clarke, 2008). Bone mass acquired during growth acts as a reservoir such that individuals with lower levels of bone mineral density (BMD) at the end of growth are at a higher risk of osteoporosis and fracture due to lower BMD levels in adulthood (Heaney et al., 2000). Bone remodelling occurs throughout life, however, after the third decade; bone resorption occurs faster than bone formation, resulting in a deficit (loss of BMD) (Bjornerem et al., 2011). Additionally, BMD is determined by both environmental and genetic factors, with a strong heritable component (Brown et al., 2005; Jouanny et al., 1995; Prentice, 2001). Measures of BMD are inversely and exponentially correlated with fracture risk, making analysis of BMD through dual energy x-ray absorptiometry (DEXA) an excellent tool for clinical diagnosis of osteoporosis (Marshall et al., 1996; Smith and Shoukri, 2000).

Because of the substantial socio-economic impact of osteoporosis globally (Gullberg et al., 1997), future studies need to address the underlying molecular and physiological mechanisms related to bone growth and the maintenance of BMD to develop better preventative and treatment options for bone loss diseases. Over the years, the insulin-like growth factor (IGF) axis has received substantial attention due to its association with bone development and maintenance as well as its potential for treatment of osteoporosis (Kasukawa et al., 2004).

1.2. Anabolic effects of Insulin like growth factor-1 (IGF-I)

IGF-I is a critical element influencing longitudinal growth, bone mass acquisition, and bone loss over multiple stages of life (Kasukawa et al., 2004; Locatelli and Bianchi, 2014). IGF-I is produced in the liver and released in circulation but is also produced locally in tissues, including bone (Cohick and Clemmons, 1993; Govoni et al., 2005; Rosen, 2004). In bone, both local and circulatory IGF-I influence growth and remodelling and the type I IGF receptor (IGF-IR) has been identified on osteoblasts as well as osteoclasts (Rosen, 2004). A proportion of homozygous *Igf1* knockout mice die shortly after birth, and surviving littermates are severely growth inhibited (Baker et al., 1993; Liu et al., 1993; Wang et al., 2006). Additionally, embryos from *Igf1* knockout mice display a delay in mineralization of bone in addition to impaired chondrocyte activity, demonstrating a role in BMD (Wang et al., 2006). Mice heterozygous for the *Igf1* knockout allele have reduced post-natal growth as well as reductions in BMD (He et al., 2006). More interestingly, mice with deletion of *Igf1* only in procollagen type II α I cells (cartilage cells) exhibit decreased longitudinal growth, lower BMD and bone mineral content as well as reductions in bone formation (Govoni et al., 2007a). Similarly, osteoblast-specific disruption of *Igf1* reduced bone size, BMD, as well as skeletal mineralization but more dramatically caused up to 50% lethality at birth (Govoni et al., 2007b), conveying that local sources are also important to healthy bone physiology. Together these studies implicate IGF-I action in processes required for longitudinal growth as well as acquisition of bone mineral density in the skeleton.

In *vitro* and clinical studies provide further evidence of the potentiating effects of IGF-I on the skeleton (Kasukawa et al., 2004). IGF-I promotes proliferation in osteoblast cultures from human and rodent origins (Canalis et al., 1989; Langdahl et al., 1998) and increases type I collagen levels while reducing collagen degradation (Canalis et al., 1995). Moreover, increases in osteoblast proliferation and markers of bone formation in response to IGF-I treatment have been observed in rat models (*in vivo*) and embryonic chick explants (*in vitro*) (Kasukawa et al., 2004; Rosen and Donahue, 1998). Consistent with the age-related occurrence of osteoporosis (Shen et al., 2003), in humans, IGF-I levels have been shown to decrease in circulation and in bone with aging (Benbassat et al., 1997; Seck et al., 1999). Moreover, IGF-I levels have been suggested to be a strong marker for early detection of bone mass changes in pre- and post-menopausal women

(Liu et al., 2008). Additional observational studies further confirm these results with a trend of decreasing IGF-I levels with age and disease state (Kasukawa et al., 2004).

Yakar *et al.*, (2010) not only demonstrates the parallels between clinical studies of IGF-I and experimental observations from mouse models, but also stresses the relevance of animal models in understanding the role of IGF-I in the skeleton (Yakar et al., 2010). Together, the *in vitro* and *in vivo* studies point towards a robust link between the anabolic effects of IGF-I and the potential for treatment of osteoporosis. Cohort studies have demonstrated a strong correlation between serum IGF-I levels and BMD as well as lower IGF-I levels in osteoporotic individuals and those with fractures (Niu and Rosen, 2005). Furthermore, a review conducted on the anabolic effects of growth hormone (GH) and the IGF-axis concluded that short-term treatment of osteoporotic or healthy individuals with recombinant human IGF-I increased bone formation in most cases and in some instances promoted bone mineral density (Kasukawa et al., 2004). However, there are certain considerations and limitations to the use of recombinant human IGF-I for treatment of osteoporosis, therefore, restricting its direct application as a therapeutic agent at this time. Some clinical studies have demonstrated that in addition to increasing markers of bone formation, short-term treatment of patients with IGF-I also increased markers of bone resorption (Ghiron et al., 1995; Johansson et al., 1992). Additionally, other clinical trials have been exploring the use of a combination of IGF-I plus another growth factor in the treatment of osteoporosis, with some reporting a positive impact on BMD (Kasukawa et al., 2004; Kawai and Rosen, 2009), and suggesting that combination treatments may be more effective than IGF-I treatment alone. Furthermore, treatment of osteoporotic patients with IGF-I and IGFBP-3 increased bone formation in a clinical trial, hinting at the use of multiple IGF components for therapy (Boonen et al., 2002). Lastly, hypoglycemia and hypophosphatemia are some of the adverse effects in response to IGF-I treatment (Kawai and Rosen, 2009); interestingly, the combination IGF-I/IGFBP-3 trial showed no side effects (Boonen et al., 2002). Because of the large scope of IGF-I action in the normal physiological state, direct application of IGF-I may not be the most effective mechanism of treating bone loss diseases.

Today, the majority of health solutions to osteoporosis involve dietary supplements and/or weight-bearing exercise to prevent bone loss, while most pharmaceutical therapies (bisphosphates, raloxifene, and nasal calcitonin) act to slow the process of skeletal

deterioration (Mauck and Clarke, 2006). Currently, the only anabolic agent being prescribed is teriparatide (Mauck and Clarke, 2006). The bisphosphates are the gold-standard for treatment of osteoporosis, acting to inhibit osteoclast activity and are considered the most effective anti-resorptive agents for prevention or treatment of osteoporosis (Mauck and Clarke, 2006; McBane, 2011). However, bisphosphates can cause esophageal irritation and/or damage, osteonecrosis of the jaw (lack of blood circulation), and musculoskeletal pain. Additionally, bisphosphates may not be suitable for patients with prior gastric or renal health conditions (Mauck and Clarke, 2006). Raloxifene is used for the prevention and treatment of postmenopausal osteoporosis and works as a selective agonist (in bone and lipid metabolism) and antagonist (in breast and uterus) to the estrogen receptor. Although effective, this drug only targets a subset of osteoporotic patients and may have dangerous side effects such as venous thromboembolism (venous blood clot) (Mauck and Clarke, 2006; McBane, 2011). Calcitonin also acts to decrease osteoclast activity, however, it has only been effective in preventing vertebral fractures (Mauck and Clarke, 2006; McBane, 2011). Estrogen and/or estrogen-progesterone therapy is only approved for prevention of osteoporosis, and not treatment. The pitfalls to hormone therapy include serious side effects such as heart disease and cancer (Mauck and Clarke, 2006). Lastly, teriparatide is a recombinant human parathyroid hormone analogue that works to promote bone formation (via osteoblast activity), and is used to treat both men and women with osteoporosis and a high risk of fracture. The major concern with teriparatide is a potential increased risk of bone cancer and it is therefore not recommended for patients who are predisposed to malignancy and/or have had extensive exposure to radiation (Mauck and Clarke, 2006).

Clearly, the current preventative and treatment options are limited and have other major negative health implications, stressing the demand for safer and more effective options to combat osteoporosis. Additionally, because of the complex roles of the IGF-axis and its components in the body, there is a need for further research to understand potential regulators of IGF-I and related anabolic pathways in order to fine tune potential drugs to target specific molecules in the system and reduce unwanted side effects while increasing the potency IGF-I action.

1.3. IGFBP-5 and PAPP-A2; IGF-regulators

In serum and bone matrix, IGFs can be found coupled to one of the six IGF-binding proteins (IGFBP-1, -2, -3, -4, -5, -6) that act as storage molecules and inhibit or facilitate IGF actions (Kasukawa et al., 2004; Locatelli and Bianchi, 2014; Rosen, 2004). Additionally, IGF-binding proteins can exhibit IGF-independent effects, adding to the complexity of processes affecting skeletal development and maintenance (Mohan and Baylink, 2002). In bone, IGFBP-5 is the predominant binding protein and has been shown to affect bone physiology through IGF-dependent and independent mechanisms (Beattie et al., 2006; Mukherjee and Rotwein, 2007). The IGF-binding proteins are in turn regulated by various enzymes that inhibit their IGF binding actions by proteolytic cleavage (Bunn and Fowlkes, 2003). Pregnancy associated plasma protein-A2 (PAPP-A2) is one such protease acting on IGFBP-5 (Overgaard et al., 2001), theoretically increasing IGF-I bioavailability. Although there is substantial evidence implicating IGFBP-5 in post-natal growth and bone mass in mice (Andress, 2001; Devlin et al., 2002; Miyakoshi et al., 2001; Salih et al., 2004; Salih et al., 2004; Salih et al., 2005), very little is known about the functions of PAPP-A2. Because PAPP-A2 potentially regulates IGF-I, exploring its role in bone physiology may help to understand the regulators of IGF-I and subsequent effects on bone mass.

This thesis aims to shed light on the function(s) of PAPP-A2 protein in bone growth and bone mineral density using three independent mouse models with constitutive, spatial (in bone), or temporal (in adulthood) deletion of the *Pappa2* gene. Constitutive *Pappa2* deletion mice lack functional PAPP-A2 protein in all tissues for the duration of their lives. The conditional *Pappa2* deletion models lack functional protein in bone or in adulthood, and acting to potentially increase IGF components in a tissue-specific or age-specific manner making my studies more advantageous than previous experiments increasing IGF components systemically.

Previous studies demonstrated that deletion of *Pappa2* reduces body mass and skeletal size (Christians et al., 2013; Conover et al., 2011). However, to understand whether *Pappa2* affects bone growth through local or systemic actions, I specifically disrupted the gene in bone using Cre-recombinase under the control of the *Ostetix* promoter (*Osx-Cre*) (Rodda and McMahon, 2006). It is predicted that the loss of PAPP-A2 would increase levels of IGFBP-5 and therefore reduce IGF-I bioavailability thus

affecting post-natal growth negatively. To assess the effects of *Pappa2* deletion on bone mineral acquisition and/or maintenance, I analyzed various morphological characteristics of bone using micro-computed tomography in constitutive *Pappa2* deletion individuals. Moreover, I analyzed biomarkers of bone formation and bone resorption in constitutive *Pappa2* deletion mice to better understand the underlying mechanisms of bone phenotypes. Because of the susceptibility of load-bearing bones to modelling in response to mass (Kular et al., 2012), I also disrupted *Pappa2* after mice had reached adulthood using a tamoxifen-induced system (Ruzankina et al., 2007) to further investigate bone phenotypes independent of body mass effects. Increasing IGFBP-5 levels has been shown to have anabolic and catabolic effects on bone (Mukherjee and Rotwein, 2007), thus it is predicted that deletion of *Pappa2* could increase or decrease BMD in deletion mice.

In addition to helping understand the basic biology of IGFBP-5 regulation, these experiments aim to shed light on potentially novel targets for osteoporosis treatment.

1.4. References

Alma Y. P, Margarita V, Lorena O, Rafael V. 2013. Molecular aspects of bone remodeling.

Andress D. 2001. IGF-binding protein-5 stimulates osteoblast activity and bone accretion in ovariectomized mice. American Journal of Physiology-Endocrinology and Metabolism 281:E283-E288.

Baker J, LIU J, Robertson E, Efstratiadis A. 1993. Role of insulin-like growth-factors in embryonic and postnatal-growth. Cell 75:73-82.

Beattie J, Allan G, Lochrie J, Flint D. 2006. Insulin-like growth factor-binding protein-5 (IGFBP-5): A critical member of the IGF axis. Biochem J 395:1-19.

Benbassat CA, Maki KC, Unterman TG. 1997. Circulating levels of insulin-like growth factor (IGF) binding protein-1 and -3 in aging men: Relationships to insulin, glucose, IGF, and dehydroepiandrosterone sulfate levels and anthropometric measures. Journal of Clinical Endocrinology & Metabolism 82:1484-1491.

Bjornerem A, Ghasem-Zadeh A, Minh Bui, Wang X, Rantzau C, Nguyen TV, Hopper JL, Zebaze R, Seeman E. 2011. Remodeling markers are associated with larger intracortical surface area but smaller trabecular surface area: A twin study. Bone 49:1125-1130.

Bonjour J, Chevalley T, Ferrari S, Rizzoli R. 2009. The importance and relevance of peak bone mass in the prevalence of osteoporosis. Salud Publica De Mexico 51:S5-S17.

Boonen S, Rosen C, Bouillon R *et al.* 2002. Musculoskeletal effects of the recombinant human IGF-I/IGF binding protein-3 complex in osteoporotic patients with proximal femoral fracture: A double-blind, placebo-controlled pilot study. Journal of Clinical Endocrinology & Metabolism 87:1593-1599.

Brown L, Streeten E, Shapiro J, McBride D, Shuldiner A, Peyser P, Mitchell B. 2005. Genetic and environmental influences on bone mineral density in pre- and post-menopausal women. Osteoporosis Int 16:1849-1856.

Bunn R, Fowlkes J. 2003. Insulin-like growth factor binding protein proteolysis. Trends in Endocrinology and Metabolism 14:176-181.

Canalis E, Centrella M, Burch W, Mccarthy TL. 1989. Insulin-like growth factor-i mediates selective anabolic effects of parathyroid-hormone in bone cultures. J Clin Invest 83:60-65.

Canalis E, Rydziel S, Delany AM, Varghese S, Jeffrey JJ. 1995. Insulin-like growth-factors inhibit interstitial collagenase synthesis in bone cell-cultures. Endocrinology 136:1348-1354.

Christians JK, de Zwaan DR, Fung SHY. 2013. Pregnancy associated plasma protein A2 (PAPP-A2) affects bone size and shape and contributes to natural variation in postnatal growth in mice. Plos One 8:e56260.

Clarke B. 2008. Normal bone anatomy and physiology. Clin J Am Soc Nephrol 3 Suppl 3:S131-9.

Cohick WS, Clemmons DR. 1993. The insulin-like growth factors. Annu Rev Physiol 55:131-153.

Conover CA, Boldt HB, Bale LK, Clifton KB, Grell JA, Mader JR, Mason EJ, Powell DR. 2011. Pregnancy-associated plasma protein-A2 (PAPP-A2): Tissue expression and biological consequences of gene knockout in mice. Endocrinology 152:2837-2844.

Devlin RD, Du Z, Buccilli V, Jorgetti V, Canalis E. 2002. Transgenic mice overexpressing insulin-like growth factor binding protein-5 display transiently decreased osteoblastic function and osteopenia. Endocrinology 143:3955-3962.

Ghiron L, Thompson J, Holloway L, Hintz R, Butterfield G, HOFFMAN A, MARCUS R. 1995. Effects of recombinant insulin-like growth-factor-i and growth-hormone on bone turnover in elderly women. Journal of Bone and Mineral Research 10:1844-1852.

Govoni K, Baylink D, Mohan S. 2005. The multi-functional role of insulin-like growth factor binding proteins in bone. Pediatr Nephrol 20:261-268.

Govoni KE, Lee SK, Chung Y, Behringer RR, Wergedal JE, Baylink DJ, Mohan S. 2007a. Disruption of insulin-like growth factor-I expression in type II alpha I collagen-expressing cells reduces bone length and width in mice. Physiological Genomics 30:354-362.

Govoni KE, Wergedal JE, Florin L, Angel P, Baylink DJ, Mohan S. 2007b. Conditional deletion of insulin-like growth factor-I in collagen type 1 alpha 2-expressing cells results in postnatal lethality and a dramatic reduction in bone accretion. Endocrinology 148:5706-5715.

Gullberg B, Johnell O, Kanis JA. 1997. World-wide projections for hip fracture. Osteoporosis Int 7:407-413.

He JN, Rosen CJ, Adams DJ, Kream BE. 2006. Postnatal growth and bone mass in mice with IGF-I haploinsufficiency. Bone 38:826-835.

Heaney R, Abrams S, Dawson-Hughes B, Looker A, Marcus R, Matkovic V, Weaver C. 2000. Peak bone mass. Osteoporosis Int 11:985-1009.

Johansson AG, Lindh E, Ljunghall S. 1992. Insulin-like growth factor-i stimulates bone turnover in osteoporosis. Lancet 339:1619-1619.

Johnell O, Kanis JA. 2006. An estimate of the worldwide prevalence and disability associated with osteoporotic fractures. Osteoporosis Int 17:1726-1733.

Jouanny P, Guillemin F, KUNTZ C, Jeandel C, Pourel J. 1995. Environmental and genetic-factors affecting bone mass - similarity of bone-density among members of healthy families. Arthritis Rheum 38:61-67.

Kasukawa Y, Miyakoshi N, Mohan S. 2004. The anabolic effects of GH/IGF system on bone. Curr Pharm Des 10:2577-2592.

Kawai M, Rosen CJ. 2009. Insulin-like growth factor-I and bone: Lessons from mice and men. Pediatric Nephrology 24:1277-1285.

Kular J, Tickner J, Chim SM, Xu J. 2012. An overview of the regulation of bone remodelling at the cellular level. Clin Biochem 45:863-873.

Langdahl BL, Kassem M, Moller MK, Eriksen EF. 1998. The effects of IGF-I and IGF-II on proliferation and differentiation of human osteoblasts and interactions with growth hormone. Eur J Clin Invest 28:176-183.

Liu J, Zhao H, Ning G, Chen Y, Zhang L, Sun L, Zhao Y, Xu M, Chen J. 2008. IGF-1 as an early marker for low bone mass or osteoporosis in premenopausal and postmenopausal women. J Bone Miner Metab 26:159-164.

Liu J, Baker J, Perkins A, Robertson E, Efstratiadis A. 1993. Mice carrying null mutations of the genes encoding insulin-like growth factor-i (igf-1) and type-1 igf receptor (Igf1r). Cell 75:59-72.

Locatelli V, Bianchi VE. 2014. Effect of GH/IGF-1 on bone metabolism and osteoporosis. International Journal of Endocrinology 235060.

Marshall D, Johnell O, Wedel H. 1996. Meta-analysis of how well measures of bone mineral density predict occurrence of osteoporotic fractures. Br Med J 312:1254-1259.

Mauck K, Clarke B. 2006. Diagnosis, screening, prevention, and treatment of osteoporosis. Mayo Clin Proc 81:662-672.

McBane S. 2011. Osteoporosis: A review of current recommendations and emerging treatment options. Formulary 46:432-+.

Miyakoshi N, Richman C, Kasukawa Y, Linkhart T, Baylink D, Mohan S. 2001. Evidence that IGF-binding protein-5 functions as a growth factor. J Clin Invest 107:73-81.

Mohan S, Baylink DJ. 2002. IGF-binding proteins are multifunctional and act via IGF-dependent and -independent mechanisms. J Endocrinol 175:19-31.

Mukherjee A, Rotwein P. 2007. Insulin-like growth factor binding protein-5 in osteogenesis: Facilitator or inhibitor? Growth Hormone & Igf Research 17:179-185.

Niu T, Rosen C. 2005. The insulin-like growth factor-I gene and osteoporosis: A critical appraisal. Gene 361:38-56.

Overgaard MT, Boldt HB, Laursen LS, Sottrup-Jensen L, Conover CA, Oxvig C. 2001. Pregnancy-associated plasma protein-A2 (PAPP-A2), a novel insulin-like growth factor-binding protein-5 proteinase. J Biol Chem 276:21849-21853.

Prentice A. 2001. The relative contribution of diet and genotype to bone development. Proc Nutr Soc 60:45-52.

Rizzoli R, Bonjour J, Ferrari S. 2001. Osteoporosis, genetics and hormones. J Mol Endocrinol 26:79-94.

Rodda SJ, McMahon AP. 2006. Distinct roles for hedgehog and canonical wnt signaling in specification, differentiation and maintenance of osteoblast progenitors. Development 133:3231-3244.

Rosen CJ, Donahue LR. 1998. Insulin-like growth factors and bone: The osteoporosis connection revisited. Proceedings of the Society for Experimental Biology and Medicine 219:1-7.

Rosen C. 2004. Insulin-like growth factor 1 and bone mineral density: Experience from animal models and human observational studies. Best Practice & Research Clinical Endocrinology & Metabolism 18:423-435.

Ruzankina Y, Pinzon-Guzman C, Asare A, Ong T, Pontano L, Cotsarelis G, Zediak VP, Velez M, Bhandoola A, Brown EJ. 2007. Deletion of the developmentallv essential gene ATR in adult mice leads to age-related phenotypes and stem cell loss. Cell Stem Cell 1:113-126.

Salih D, Kasukawa Y, Tripathi Q, Lovett F, Anderson N, Carter E, Wergedal J, Baylink J, Pell J, Mohan S. 2004. Transgenic overexpression of IGFBP-5 in mice leads to unexpected decrease in peak BMD in a gender specific manner: Evidence for IGF-independent mechanism of action. Journal of Bone and Mineral Research 19:S47-S47.

Salih D, Mohan S, Kasukawa Y, Tripathi G, Lovett F, Anderson N, Carter E, Wergedal J, Baylink D, Pell J. 2005. Insulin-like growth factor-binding protein-5 induces a gender-related decrease in bone mineral density in transgenic mice. Endocrinology 146:931-940.

Salih D, Tripathi G, Holding C, Szestak T, Gonzalez M, Carter E, Cobb L, Eisemann J, Pell J. 2004. Insulin-like growth factor-binding protein 5 (Igfbp5) compromises survival, growth, muscle development, and fertility in mice. Proc Natl Acad Sci U S A 101:4314-4319.

Seck T, Bretz A, Krempien R, Krempien B, Ziegler R, Pfeilschifter J. 1999. Age-related changes in insulin-like growth factor I and II in human femoral cortical bone: Lack of correlation with bone mass. Bone 24:387-393.

Shen H, Recker RR, Deng HW. 2003. Molecular and genetic mechanisms of osteoporosis: Implication for treatment. Curr Mol Med 3:737-757.

Smith J, Shoukri K. 2000. Diagnosis of osteoporosis. Clin Cornerstone 2:22-33.

Viguet-Carrin S, Garnero P, Delmas P. 2006. The role of collagen in bone strength. Osteoporosis Int 17:319-336.

Wang Y, Nishida S, Sakata T, Elalieh HZ, Chang W, Halloran BP, Doty SB, Bikle DD. 2006. Insulin-like growth factor-I is essential for embryonic bone development. Endocrinology 147:4753-4761.

Yakar S, Courtland H, Clemmons D. 2010. IGF-1 and bone: New discoveries from mouse models. Journal of Bone and Mineral Research 25:2267-2276.

Chapter 2.

PAPP-A2 expression by osteoblasts is required for normal postnatal growth in mice

2.1. Background

Insulin-like growth factors (IGFs) are peptide hormones with both systemic and local effects (Cohick and Clemmons, 1993). IGF binding proteins (IGFBPs) bind IGFs with high affinity, prolonging their half-lives and assisting or inhibiting the interaction of IGFs with their receptors, thereby modulating their bioavailability (Mohan and Baylink, 2002). The IGF axis is an important regulator of bone physiology (Govoni et al., 2005; Mohan et al., 2003). In osteoblasts, IGFs influence cellular proliferation, differentiation, and apoptosis through autocrine and paracrine signalling and are required for bone development, mineral deposition, and skeletal growth (Govoni et al., 2005; Zhang et al., 2012). IGFBP-5 is the most abundant IGFBP in bone and affects bone processes through IGF-dependent and -independent pathways (Miyakoshi et al., 2001; Mohan and Baylink, 2002). In mice, transgenic IGFBP-5 over-expression causes a decrease in bone mineral density (Atti et al., 2005; Devlin et al., 2002; Salih et al., 2005), inhibits whole-body and muscle growth, increases the risk of neonatal death, and decreases fertility (Salih et al., 2004).

The IGFBPs are themselves regulated by proteases (Bunn and Fowlkes, 2003; Govoni et al., 2005). Pregnancy associated plasma protein-A and –A2 (PAPP-A and PAPP-A2) are IGFBP proteases which share 45% sequence identity (Overgaard et al., 2001). PAPP-A is a biomarker of pregnancy diseases (Christians and Gruslin, 2010) and cardiovascular complications (Kaski and Holt, 2006), and has been implicated in bone growth and the maintenance of bone mineral content (Conover et al., 2004; Tanner et al., 2008). In contrast, little is known about PAPP-A2. Since PAPP-A cleaves IGFBP-4 and -5, while PAPP-A2 acts upon IGFBP-5 (Overgaard et al., 2001), deletion of *Pappa* or *Pappa2* would be expected to increase levels of intact IGFBP-5 and potentially have similar consequences to transgenic IGFBP-5 over-expression. Indeed, *Pappa* deletion mice have reduced body mass and bone lengths and lower bone mineral density compared to wild-type mice (Tanner et al., 2008). Similarly, *Pappa2* deletion mice exhibit

reduced postnatal growth (Conover et al., 2011), with bone lengths reduced more than would be expected given the reduction in body mass alone (Christians et al., 2013). Additionally, natural variation in the *Pappa2* gene contributes to variation in skeletal growth in mice (Christians et al., 2006; Christians et al., 2013).

Although these studies indicate that PAPP-A2 plays a role in postnatal growth, it is not known whether PAPP-A2 acts in a local or systemic manner, i.e., are effects of PAPP-A2 on bone and IGFBP-5 bioavailability due to locally produced PAPP-A2, and/or PAPP-A2 produced elsewhere? I hypothesized that bone-derived PAPP-A2 plays a role in post-natal skeletal development. To determine whether PAPP-A2 has primarily local or systemic effects, *Pappa2* was deleted specifically in osteoblasts by crossing conditional *Pappa2* deletion mice with mice expressing *Cre* recombinase under the control of the *Osterix* (*Osx/Sp7*) promoter (Rodda and McMahon, 2006). Furthermore, I sought to characterize PAPP-A2 expression in the long bones using immunohistochemistry.

2.2. Methods

2.2.1. Ethics Statement

All work was carried out in accordance with the guidelines of the Canadian Council on Animal Care and was approved by the SFU University Animal Care Committee (protocol 1035B-11).

2.2.2. *Pappa2* deletion mice

Conditional *Pappa2* deletion mice with a C57BL/6 background were generated as previously described (Christians et al., 2013), such that mouse exon 2 (homologous to human exon 3) and a PGK-Neo selection cassette were flanked by LoxP sites (i.e., “floxed”). The selection cassette was flanked by FRT sequences and was removed by breeding with mice carrying a *Flp* recombinase transgene (Jackson Laboratory stock number 011065). Following *Flp* recombinase mediated removal of the selection cassette, the *Flp* recombinase transgene was removed by further breeding to produce mice with a floxed exon 2 and no selection cassette or *Flp* transgene. Osteoblast-specific deletion of exon 2 was achieved by crossing conditional deletion mice to mice expressing *Cre*

recombinase under the control of the Osterix (*Osx/Sp7*) promoter (hereafter referred to as *Osx-Cre*; Jackson Laboratory stock number 006361). Cre-mediated deletion of exon 2 and splicing of exon 1 to exon 3 is expected to produce an early stop codon, and has been previously shown that this results in PAPP-A2 protein being undetectable in the placenta, despite being abundant in wild-type mice (Christians et al., 2013).

To determine whether floxing *per se* affected PAPP-A2 protein levels, mice heterozygous for the conditional *Pappa2* allele (*Pappa2*$^{wt/fl}$) were paired to produce pregnancies in which embryos of all three genotypes were present: homozygous for the conditional *Pappa2* allele (*Pappa2*$^{fl/fl}$), homozygous wild-type (*Pappa2*$^{wt/wt}$), and heterozygous (*Pappa2*$^{wt/fl}$). PAPP-A2 protein was then measured in the placenta by Western blotting (described below). Females were checked for seminal plugs the morning following pairing, and plugged females were euthanized with CO_2 twelve days later, i.e., embryonic day 12.5 (E12.5). Females were collected at E12.5 to ensure that individual placentae would be sufficiently large for protein extraction and because PAPP-A2 expression is high at this stage (Wang et al., 2009). Placentae were dissected while immersed in phosphate buffered saline (PBS), weighed, and frozen at -80°C for quantification of protein levels by Western blotting. The amniotic sac and/or a piece of embryonic tail were collected for PCR genotyping. In total, 8 placentae from 2 female mothers were obtained for protein analysis including 2 *Pappa2*$^{wt/wt}$, 4 *Pappa2*$^{wt/fl}$, and 2 *Pappa2*$^{fl/fl}$ samples.

To determine the effect of osteoblast-specific *Pappa2* deletion, mice heterozygous for the conditional *Pappa2* allele and hemizygous for the *Osx-Cre* transgene (*Pappa2*$^{wt/fl}$;*Osx-Cre*) were paired with mice homozygous for the conditional *Pappa2* allele with no transgene (*Pappa2*$^{fl/fl}$) to produce litters in which four genotypes were present: homozygous or heterozygous for the conditional *Pappa2*^{fl} allele and with or without the *Osx-Cre* transgene. Previous work in the Christians lab suggested that the effects of constitutive *Pappa2* deletion on growth are recessive (Christians et al., 2013), therefore I expected to detect effects of osteoblast-specific deletion by comparing homozygotes and heterozygotes expressing the *Osx-Cre* transgene. These offspring were used for measurement of postnatal growth (described below). Removal of *Pappa2* exon 2 in bone was determined by PCR genotyping (described below). Postnatal growth was measured in 46 males and 40 females.

2.2.3. Constitutive *Pappa2* deletion mice

Constitutive PAPP-A2 deletion mice were produced in a previous study (Christians et al., 2013) and were used to compare the effects of osteoblast-specific *Pappa2* deletion (this study) with the effects of whole-body *Pappa2* deletion. Briefly, conditional deletion mice were crossed to mice expressing *Cre* recombinase under the control of a human cytomegalovirus minimal promoter (Jackson Laboratory stock number 006054). Mice heterozygous for the constitutive *Pappa2* disruption were then paired to produce litters in which all three genotypes were present (i.e., $Pappa2^{wt/wt}$, $Pappa2^{wt/KO}$, $Pappa2^{KO/KO}$) resulting in 40 male and 35 female offspring.

2.2.4. Genotyping

Mice were ear-clipped at three weeks of age and extraction of DNA was performed by standard methods. PCR genotyping was used for the determination of (a) *Pappa2* alleles, i.e., $Pappa2^{wt}$, $Pappa2^{fl}$, and $Pappa2^{KO}$, and (b) the presence/absence of the *Osx-Cre* transgene. Genotyping of *Pappa2* alleles used three primers designed to yield bands of different sizes for the three alleles (166 bp for $Pappa2^{wt}$, 305 bp for $Pappa2^{fl}$ and 272 bp for $Pappa2^{KO}$). Primer sequences are as follows:

KO_prox (5'-CAGCAAAGGAAATTTGTGCT-3'),
KO_exon2 (5'-GGTCAAATGAAACTTCCCTCC-3'),
KO_dist2 (5'-CTCTTGCATGCCTCCACTAC-3').

The genotyping reactions for *Osx-Cre* included two primer pairs recommended by the Jackson Laboratory: one to amplify a fragment from the *Osx-Cre* transgene and another to amplify a positive control fragment to confirm that the PCR was successful. The positive control primers target an exon of the *Interleukin 2* gene on chromosome 3. Primer sequences are as follows:

Cre_A (5'-GCGGTCTGGCAGTAAAAACTATC-3'),
Cre_B (5'-GTGAAACAGCATTGCTGTCACTT-3'),
Cre_+ve_A (5'-CTAGGCCACAGAATTGAAAGATCT-3'),
Cre_+ve_B (5'-GTAGGTGGAAATTCTAGCATCATCC-3').

2.2.5. Phenotypes

Body mass and tail length were measured at 3, 6, 10, and 12 weeks of age in offspring from the cross between *Pappa2*$^{wt/fl}$; *Osx-Cre* and *Pappa2*$^{fl/fl}$ mice. Mice were sacrificed at 12 weeks of age and frozen at -20°C. These mice were thawed at a later date, the skin and internal organs were removed and the carcasses were dried to a constant weight before being exposed to dermestid beetles for removal of soft tissue, allowing the following bone measurements: mandible length (distance from the tip of the angular process to the anterior edge of the molars), mandible height (from the coronoid process to the tip of the angular process), and the lengths of the skull, humerus, ulna/radius, femur, tibia, and pelvic girdle. Where applicable, bones were measured from both sides and the mean was calculated. All skeletal dimensions were measured with digital callipers (± 0.01 mm) and measurements were performed in triplicate. To confirm bone-specific *Pappa2* disruption in *Pappa2*$^{fl/fl}$; *Osx-Cre* mice, some mice were sacrificed at 6 weeks of age to collect tissues for genotyping and bones for Western blotting. Samples of ear, bone, heart, liver, lung, kidney, spleen, and muscle were collected and stored at -80°C. Tissues were extracted using the DNeasy Blood & Tissue Kit (Cat. No. 69504) from Qiagen (Hilden). PCR was performed using standard methods to determine the presence or absence of the 272 bp deletion allele in these samples.

2.2.6. Protein extraction and Western

Placentae and bones were homogenized in 2 mL (placentae) or 1.5 mL (bone) of T-PER™ Tissue Protein Extraction Reagent (PIERCE, Rockford, IL), incubated on ice for 7 minutes and centrifuged at 10,000 g for 5 minutes at 4°C. The supernatant was collected and stored at -20°C. Placental or bone samples containing 62.5 µg or 121 µg of protein, respectively, were mixed with SDS loading buffer, boiled and run through a 4% stacking and 8% or 12% separating polyacrylamide gel (PAPP-A2 or IGFBP-5, respectively) for 60 minutes. The gel was equilibrated in transfer buffer and transferred onto a nitrocellulose membrane (Bio-Rad, Hercules, CA). Membranes were blocked for one hour at room temperature in Odyssey Blocking Buffer (Li-Cor Biosciences, Lincoln, Nebraska), incubated for one hour (for placentae) or overnight at 4°C (for bone) in a solution containing 1:500 monoclonal mouse anti-actin (CLT9001; Cedarlane, Burlington ON) and 1:500 polyclonal goat-anti-human PAPP-A2 antibody (AF1668; R&D Systems, Minneapolis, MN) or 1:500 polyclonal goat-anti mouse IGFBP-5 (AF578; R&D Systems)

diluted in Odyssey Blocking Buffer (Li-Cor Biosciences, Lincoln, NE) and 0.1% Tween-20 (Sigma, ON, Canada), washed 5 times, and incubated in a solution containing 1:10000 fluorescently-labelled IRDye 800 anti-goat and IRDye 680 anti-mouse secondary antibodies (Li-Cor Biosciences, Lincoln, NE) diluted in Odyssey Blocking Buffer, 0.1% Tween-20 and 0.1% SDS for 45 minutes with gentle shaking. The membranes were again washed 5 times. Membranes were visualized using the Odyssey infrared imaging system (Li-Cor Biosciences, Lincoln, NE). The two secondary dyes fluoresce at different wavelengths, allowing for simultaneous quantification of the intensity of the PAPP-A2 band (at approximately 250 kDa) and the actin band (at approximately 40 kDa) or the IGFBP-5 band (approximately 35 kDa) and the actin band on the same nitrocellulose membrane.

2.2.7. Measurement of circulating IGFBP-5 levels

Plasma levels of IGFBP-5 in 16 juvenile (18-19 day old) mice were determined by ELISA (DY578; R&D Systems).

2.2.8. Immunohistochemistry

Long bones were dissected at 8 weeks (young adult mice) and 19 days (juvenile mice) in cold PBS. All soft tissues were carefully removed and samples fixed in 10% neutral buffered formalin for 72 hours. Femoro-tibial joints were subsequently decalcified in 10% EDTA and embedded in paraffin. Sections were deparaffinised and rehydrated according to standard protocols and heat-antigen retrieval was performed in 10mM citrate buffer pH 6.0. Immunohistochemistry was performed using HRP-AEC (CTS009; R&D Systems). Sections were incubated overnight at 4°C with 10 µg/mL of polyclonal goat-anti-human PAPP-A2 antibody (AF1668; R&D Systems) or 5 µg/mL of polyclonal goat-anti mouse IGFBP-5 (AF578; R&D Systems) or matched concentrations of normal goat IgG control (AB-108-C; R&D Systems) as a negative control. Sections were counterstained using Gills No. 3 Hematoxylin diluted 1:5 in sterile water. All experiments were performed in duplicate on sections from 4 young adult (3 *Pappa2*$^{fl/fl}$ and 1 *Pappa2*$^{fl/fl}$*;Osx-Cre*) and 7 juvenile (3 *Pappa2*$^{fl/fl}$ and 4 *Pappa2*$^{fl/fl}$*; Osx-Cre*) mice. The intensity of PAPP-A2 staining in osteoblasts of juvenile mice was scored by two individuals blind to genotype.

2.2.9. Statistical Analyses

All statistical analyses were performed using general linear models (proc GLM) and repeated measures analyses (proc MIXED) in SAS, Version 9.3 (SAS Institute Inc., Cary, NC).

2.3. Results

2.3.1. Effects of floxing on PAPP-A2 protein expression in the placenta

To assess potential effects of floxing on PAPP-A2 protein expression, *Pappa2*$^{wt/fl}$ mice were paired to produce pregnancies in which embryos and placentae of all three genotypes (*Pappa2*$^{fl/fl}$, *Pappa2*$^{wt/wt}$, and *Pappa2*$^{wt/fl}$) were present. PAPP-A2 protein expression levels did not differ between genotypes in E12.5 placentae (Fig. 2.1).

2.3.2. *Pappa2* deletion in bone

Deletion of *Pappa2* in bone was determined using PCR targeting the 272 bp deletion allele. In *Pappa2*$^{fl/fl}$;*Osx-Cre* mice, PCR of DNA from ear-clip, liver, lung, heart, muscle, kidney, spleen and bone yielded the deletion band only in bone samples (Fig. 2.2) when using only the KO_prox and KO_dist2 primers (which amplified the *Pappa2*^{KO} allele but not the *Pappa2*^{fl} allele). In contrast, when all three primers were used, the *Pappa2*^{fl} allele could be detected in all samples, whereas the *Pappa2*^{KO} allele was not detected in any (data not shown). In the PCR with all three primers, it is likely that the *Pappa2*^{fl} allele outcompeted the *Pappa2*^{KO} allele because *Pappa2* was not disrupted in most cell types. PAPP-A2 protein was detectable in femoral extracts by Western blotting at very low levels, but I did not detect a difference in expression between control and osteoblast-specific deletion samples (data not shown), presumably because the low protein levels precluded accurate quantification and/or because other cell types expressed PAPP-A2.

In the femur and tibia, immunostaining for PAPP-A2 was present in the epiphysis and metaphysis (Fig. 2.3). Staining was also observed in osteoblasts (Fig. 2.3). Blind scoring of immunohistochemistry images revealed a trend of reduced/absent staining in osteoblasts of *Pappa2*$^{fl/fl}$*;Osx-Cre* mice (Fig. 2.4), although *Osx-Cre*-mediated deletion did not appear to be complete.

To determine whether PAPP-A2 levels affected IGFBP-5 levels, Western analysis and immunohistochemistry were performed on bone samples of adult and juvenile mice. Immunohistochemistry revealed that IGFBP-5 localization overlaps that of PAPP-A2 in the femoro-tibial joint (Fig. 2.3). IGFBP-5 and PAPP-A2 were detectable using Western

blotting, but there were no differences in protein levels between genotypes. PAPP-A2 and IGFBP-5 expression was higher in juvenile bones compared to young adult bones and this difference was observed in both Western blots and immunohistochemistry (data not shown).

2.3.3. Plasma IGFBP-5

In a model including effects of litter, *Pappa2* genotype, *Osx-Cre* genotype and the interaction between *Pappa2* and *Osx-Cre* genotype, plasma IGFBP-5 levels were significantly reduced in 18-19 day old mice carrying the *Osx-Cre* transgene ($F_{1,9}$= 26.86, P=0.0006) (Fig. 2.5). However, there was no difference in IGFBP-5 levels between *Pappa2* genotypes ($F_{1,9}$= 0.23, P=0.64) and the statistical interaction between *Pappa2* and *Osx-Cre* genotype was not significant ($F_{1,9}$=0.18, P= 0.69). Sex was initially included in the model but was not significant.

2.3.4. Effects of osteoblast-specific *Pappa2* deletion

In offspring of *Pappa2*$^{wt/fl}$;*Osx-Cre* and *Pappa2*$^{fl/fl}$ mice, genotypic ratios deviated from the expected Mendelian values. The numbers of *Pappa2*$^{wt/fl}$: *Pappa2*$^{fl/fl}$: *Pappa2*$^{wt/fl}$*;Osx-Cre*: *Pappa2*$^{fl/fl}$*;Osx-Cre* mice were 34, 25, 22,15, respectively, which significantly deviated from the expected ratio of 1:1:1:1 (χ^2_3=7.75, p=0.005). In addition, the ratio of offspring that inherited the *Osx-Cre* transgene to those that did not was 37:59, which deviated from the expected 1:1 ratio (χ^2_1=5.04, p=0.02). The deficiency of mice carrying the *Osx-Cre* transgene, particularly among those with the *Pappa2*$^{fl/fl}$ genotype, suggests an effect of the transgene on survival. Mice with osteoblast-specific *Pappa2* disruption may have been more susceptible, perhaps because of reduced size (see below).

Osteoblast-specific *Pappa2* deletion effects were examined by measuring body mass and tail lengths at 3, 6, 10 and 12 weeks of age and measuring linear bone dimensions after cull at 12 weeks of age. I predicted that postnatal growth would be reduced in *Pappa2*$^{fl/fl}$;*Osx-Cre* mice compared to *Pappa2*$^{wt/fl}$;*Osx-Cre* mice due to deletion of *Pappa2* in osteoblasts, but that there would be no difference between *Pappa2*$^{fl/fl}$ and *Pappa2*$^{wt/fl}$ mice not carrying the *Osx-Cre* transgene, i.e., I predicted an interaction between the *Pappa2* allele genotype and the *Cre* genotype. Combining measures from

all ages using MANOVA, the statistical interaction between the *Pappa2* allele genotype and the *Osx-Cre* genotype was significant for body mass (Wilks' Lambda F4,68 = 3.75; P = 0.0082) and tail length (Wilks' Lambda F4,69 = 3.34; P = 0.0148). Similarly, the interaction was also significant in the repeated measures analysis of body mass ($F_{1,72}$=12.78; P=0.0006) and tail length ($F_{1,72}$=6.23; P=0.0148). To determine the nature of the interaction, the CONTRAST statement in proc GLM was used to compare the least squares means for the *Pappa2*$^{fl/fl}$ and *Pappa2*$^{wt/fl}$ genotypes separately for mice with and without the *Osx-Cre* transgene. For body mass and tail length at all ages, the differences between *Pappa2* genotypes were significant for mice with the *Osx-Cre* transgene, and not significant for mice without the *Osx-Cre* transgene (Table 2.1 and Fig. 2.6). The *Osx-Cre* transgene also reduced body size independent of the *Pappa2* allele genotype (Fig. 2.6), as previously found by Davey et al. (Davey et al., 2012). There were no significant interactions between sex and *Pappa2* and/or *Osx-Cre* genotype, i.e., the effects of *Pappa2* deletion were not sex-specific.

Similar results for linear bone dimensions were observed (Table 2.1 and Fig. 2.6). There was a significant interaction between the *Pappa2* allele genotype and the *Osx-Cre* genotype for bones of the head (skull and mandible dimensions; MANOVA Wilks' Lambda F3,53 = 8.72; P = 0.0001) and the long bones (humerus, radius/ulna, femur and tibia; MANOVA Wilks' Lambda F4,69 = 3.40; P = 0.0135). As with body mass and tail length, in all bones there was a significant difference between *Pappa2* genotypes in mice with the *Osx-Cre* transgene, but not in mice without the *Osx-Cre* transgene (Table 2.1 and Fig. 2.6). Interactions between sex and genotype were initially included in models, but were not found to be significant for any trait, i.e., the effects of *Pappa2* deletion were not sex-specific.

2.3.5. Comparison of effects of osteoblast-specific and constitutive *Pappa2* deletion

To compare the effects of osteoblast-specific and constitutive *Pappa2* deletion, the phenotypic data from the present study were combined with that from a previous study of constitutive *Pappa2* deletion (Christians et al., 2013). Phenotypes were analysed using a general linear model including the effects of experiment (i.e., osteoblast-specific or constitutive deletion), genotype (*Pappa2*$^{wt/fl}$, *Pappa2*$^{fl/fl}$, *Pappa2*$^{wt/fl}$*;Osx-Cre,* *Pappa2*$^{fl/fl}$*;Osx-Cre*; *Pappa2*$^{wt/wt}$, *Pappa2*$^{wt/KO}$, *Pappa2*$^{KO/KO}$, nested within experiment),

litter identity (nested within experiment), and sex. In this analysis, I aimed to test whether the effect of osteoblast-specific deletion (i.e., *Pappa2*$^{wt/fl}$*;Osx-Cre* vs. *Pappa2*$^{fl/fl}$*;Osx-Cre*) was different than the effect of constitutive deletion (i.e., *Pappa2*$^{wt/KO}$ vs. *Pappa2*$^{KO/KO}$; heterozygotes were compared to homozygotes because this was the comparison in the osteoblast-specific experiment). Differences between genotypes were estimated using ESTIMATE statements, and the difference between estimates was tested using a CONTRAST statement in proc GLM. Even though the contrast only involved 4 of the 7 genotypes, all genotypes were included in the general linear model to improve the estimation of the effects of sex and litter identity. Prior to this analysis, all phenotypes were standardized within each experiment by subtracting the mean and dividing by the standard deviation of the *Pappa2*$^{wt/fl}$*;Osx-Cre* mice (osteoblast-specific experiment) or the *Pappa2*$^{wt/KO}$ mice (constitutive experiment). As a result, the *Pappa2*$^{wt/fl}$*;Osx-Cre* mice and the *Pappa2*$^{wt/KO}$ mice had a mean of 0 and a standard deviation of 1 for every phenotype, and the phenotypes of all mice were expressed in standard deviation units. The rationale for this standardization was twofold. First, expressing the data as standard deviation units allows comparison of the magnitude of effects between traits. Second, the *Pappa2*$^{wt/fl}$*;Osx-Cre* mice are smaller than the *Pappa2*$^{wt/KO}$ mice because of the *Cre* transgene. Therefore, without standardization, a difference of 1 gram or millimeter between the *Pappa2*$^{wt/fl}$*;Osx-Cre* and *Pappa2*$^{fl/fl}$*;Osx-Cre* mice would represent a proportionately greater effect than the same absolute difference between the *Pappa2*$^{wt/KO}$ and *Pappa2*$^{KO/KO}$ mice. For body mass at 10 weeks, tail length at 3, 6 and 10 weeks, mandible dimensions and the length of the femur, the difference between *Pappa2*$^{wt/KO}$ and *Pappa2*$^{KO/KO}$ mice was significantly greater than the difference between *Pappa2*$^{wt/fl}$*;Osx-Cre* and *Pappa2*$^{fl/fl}$*;Osx-Cre* mice, i.e., the effect of constitutive PAPP-A2 deletion was greater than the effects of osteoblast-specific deletion (Table 2.2). For 6 week body mass, the estimated effect of constitutive deletion was substantially greater than the effect of osteoblast-specific deletion, and the difference between these effects was marginally non-significant ($P = 0.09$). For body mass at 3 weeks, and the measurements of all bones apart from the mandible and femur, there was no significant difference between the estimated effects of the constitutive and osteoblast-specific deletion (Table 2.2).

2.4. Discussion

This study is the first to investigate the role of bone-derived PAPP-A2 using *Osterix* (*Osx/Sp7)* driven *Cre* recombinase expression, a method previously used for osteoblast-specific gene disruption (Rodda and McMahon, 2006). I detected the *Pappa2* deletion allele in bone only, although some *Cre* expression in the brain, intestinal epithelium, and olfactory cells has been reported with this transgene (Chen et al., 2014; Davey et al., 2012). To assess the phenotypic consequences of *Osx-Cre*-driven *Pappa2* disruption, *Pappa2*$^{wt/fl}$;*Osx-Cre* mice were mated with *Pappa2*$^{fl/fl}$ mice lacking *Cre* to produce offspring homozygous or heterozygous for the conditional *Pappa2* allele, with or without the *Osx-Cre* transgene. Offspring genotypes deviated from expected Mendelian ratios such that *Pappa2*$^{fl/fl}$*;Osx-Cre* mice were under-represented, potentially due to high mortality of very small fetuses or pups. I found a significant interaction between the *Pappa2* and *Osx-Cre* genotypes for all traits, such that there was a difference between *Pappa2* genotypes only when the *Osx-Cre* transgene was present, i.e., homozygous conditional deletion mice were smaller than heterozygous littermates.

Osteoblast-specific disruption of *Pappa2* resulted in a significant decrease in body mass and skeletal size at all ages, suggesting that osteoblast-produced PAPP-A2 affects postnatal growth of bones and other tissues. The phenotypic difference between constitutive knock-outs and controls (*Pappa2*$^{KO/KO}$ vs. *Pappa2*$^{wt/KO}$) was more pronounced than that between osteoblast-specific deletion mice and controls (*Pappa2*$^{fl/fl}$*;Osx-Cre* vs. *Pappa2*$^{wt/fl}$*;Osx-Cre*) for body mass, tail length, mandible dimensions and femur length, indicating that postnatal growth is affected by PAPP-A2 produced by other tissues as well as that produced by bone. However, the underrepresentation of the *Pappa2*$^{fl/fl}$*;Osx-Cre* genotypes suggests that the smallest of these mice may have died before weaning, in which case the effects of osteoblast-specific *Pappa2* deletion are likely to be underestimated in the present study. In the previous study of constitutive *Pappa2* deletion mice (Christians et al., 2013), genotypes did not differ from the expected Mendelian ratios, perhaps because the reduction in body size caused by *Pappa2* deletion was not exacerbated by a reduction due to the presence of the *Osx-Cre* transgene.

Blind-scoring of PAPP-A2 staining in osteoblasts of *Pappa2*$^{fl/fl}$;*Osx-Cre* mice confirmed reduced levels, but suggested that disruption was incomplete, perhaps due to variable *Osx-Cre* expression. Furthermore, since PAPP-A2 is a secreted protein, the

possibility that the PAPP-A2 detected was produced elsewhere and bound to osteoblasts cannot be ruled out.

Plasma IGFBP-5 levels were not lower in *Pappa2*$^{fl/fl}$;*Osx-Cre* mice, suggesting that even local IGFBP-5 changes can have a substantial effect on growth. Whether local PAPP-A2 exerts effects through IGF-dependent and/or IGF-independent actions of IGFBP-5 remains unknown. While circulating IGF-I influences bone development and physiology, locally-produced IGF-I is also important (Yakar et al., 2010). Deletion of IGF-I in chondrocytes reduces bone growth, bone mineral density, and *Igfbp5* expression (Govoni et al., 2007a). Similarly, osteocyte-specific IGF-I deletion mice show decreases in developmental bone growth and a reduction in bone formation parameters (Sheng et al., 2013). More dramatically, mice lacking IGF-I in collagen type 1α2 expressing cells (i.e., osteoblast lineage) exhibit postnatal lethality, reduction in body mass and bone size as well as decreases in bone mineral density (Govoni et al., 2007b). The phenotypic effects of bone cell-specific IGF-I deletion suggest that locally-produced IGF-I is critical for postnatal bone physiology. IGFBP-5 regulates IGF-I availability and inhibits IGF-I action in bone (Mukherjee and Rotwein, 2008), but also has IGF-independent effects (Beattie et al., 2006). Furthermore, a recent study in zebrafish has linked PAPP-A2 to pathways outside the IGF system (Kjaer-Sorensen et al., 2014), raising the possibility that the effects I observed could have been due to IGFBP-5-independent effects. However, the effects of PAPP-A2's paralog, PAPP-A, in bone appear to be due to its IGFBP proteolytic activity. Transgenic overexpression of PAPP-A in bone affects a number of bone parameters (Qin et al., 2006), and these effects are abolished in mice that also express a protease-resistant IGFBP-4 analog in bone (Phang et al., 2010).

PAPP-A2 localization was characterized in long bones and the pattern of immunoreactivity was compared with that of IGFBP-5 using immunohistochemistry. I show localization of PAPP-A2 and IGFBP-5 in the epiphysis and metaphysis as well as the osteoblasts. PAPP-A2 immunoreactivity overlapped with that of IGFBP-5 in the long bones, consistent with the enzyme-substrate relationship. Co-localization of the IGFs at the growth plate (Parker et al., 2007) with PAPP-A2 and IGFBP-5 in close proximity reflects the importance of this pathway for longitudinal growth.

Overall, this chapter documents PAPP-A2 expression in the long bones and demonstrates that both osteoblast-produced and other sources of PAPP-A2 are important

for post-natal growth in mice. However, the loss of *Pappa2*$^{fl/fl}$;*Osx-Cre* individuals (potentially due to combined effects of *Pappa2* deletion and the *Osx-Cre* transgene on growth), may have resulted in an underestimation of phenotypic effects. The co-localization of IGFBP-5 and PAPP-A2 supports my hypothesis that local PAPP-A2 is important to postnatal growth, either through proteolysis of local IGFBP-5 and increased IGF-I bioavailability, IGF-independent pathways, or even as yet unstudied IGFBP-5 independent pathways.

2.5. Tables and Figures

Table 2.1. Effects of osteoblast-specific *Pappa2* deletion on postnatal growth.

Trait	*Pappa2*$^{fl/fl}$; *Osx-Cre*+	*Pappa2*$^{wt/fl}$;*Osx-Cre*+	*Pappa2*$^{fl/fl}$;*Osx-Cre*-	*Pappa2*$^{wt/fl}$;*Osx-Cre*-	P value (*Pappa2*Cre* interaction)	P value (*Cre*+ contrast)	P value (*Cre*- contrast)
3 week mass (g)	6.7 ± 0.3	7.8 ± 0.3	9.1 ± 0.3	9.0 ± 0.2	0.021	0.010	0.70
3 week tail length (cm)	5.2 ± 0.1	5.5 ± 0.1	5.7 ± 0.1	5.7 ± 0.1	0.049	0.037	0.63
6 week mass (g)	15.5 ± 0.5	17.0 ± 0.4	19.1 ± 0.4	18.9 ± 0.3	0.025	0.014	0.67
6 week tail length (cm)	7.0 ± 0.1	7.2 ± 0.1	7.4 ± 0.1	7.5 ± 0.1	0.095	0.029	0.90
10 week mass (g)	19.2 ± 0.6	20.8 ± 0.5	22.6 ± 0.5	22.3 ± 0.4	0.054	0.043	0.56
10 week tail length (cm)	7.8 ± 0.1	8.1 ± 0.1	8.1 ± 0.1	8.1 ± 0.1	0.002	0.001	0.43
12 week mass (g)	20.4 ± 0.6	22.2 ± 0.4	23.7 ± 0.4	23.1 ± 0.3	0.007	0.009	0.25
12 week tail length (cm)	8.0 ± 0.1	8.2 ± 0.1	8.2 ± 0.1	8.2 ± 0.1	0.055	0.025	0.79
Mandible length (mm)	7.9 ± 0.1	8.3 ± 0.1	8.9 ± 0.1	8.8 ± 0.1	0.008	0.002	0.72
Mandible height (mm)	5.6 ± 0.1	6.0 ± 0.1	6.6 ± 0.1	6.5 ± 0.1	0.005	0.002	0.56
Skull (mm)	20.9 ± 0.2	22.2 ± 0.1	22.9 ± 0.1	22.8 ± 0.1	0.001	0.001	0.38
Humerus (mm)	11.1 ± 0.1	11.5 ± 0.1	11.7 ± 0.1	11.7 ± 0.1	0.003	0.001	0.57
Ulna/Radius (mm)	13.0 ± 0.1	13.3 ± 0.1	13.6 ± 0.1	13.6 ± 0.1	0.007	0.002	0.67
Femur (mm)	13.7 ± 0.1	14.2 ± 0.1	14.5 ± 0.1	14.4 ± 0.1	0.002	0.001	0.37
Tibia (mm)	16.0 ± 0.1	16.5 ± 0.1	17.0 ± 0.1	17.0 ± 0.1	0.001	0.001	0.62
Pevlic girdle (mm)	17.7 ± 0.1	18.6 ± 0.1	18.7 ± 0.1	18.7 ± 0.1	0.001	0.001	0.97

Values are least square means (± standard error), controlling for the effects of sex and litter identity.

Table 2.2. Comparison of phenotypic effects of constitutive and osteoblast-specific *Pappa2* deletion.

Trait	Sample sizes				Difference between *Pappa2*$^{wt/KO}$ and *Pappa2*$^{KO/KO}$	Difference between *Pappa2*$^{wt/fl}$; *Osx-Cre* and *Pappa2*$^{fl/fl}$; *Osx-Cre* mice	P-value for contrast between constitutive and osteoblast-specific effect
	Pappa2$^{wt/KO}$	*Pappa2*$^{KO/KO}$	*Pappa2*$^{wt/fl}$;*Osx-Cre*	*Pappa2*$^{fl/fl}$;*Osx-Cre*			
3 week mass	53	24	22	15	0.48 ± 0.15	0.56 ± 0.20	0.74
3 week tail length	16	8	22	15	1.14 ± 0.31	0.38 ± 0.24	0.05
6 week mass	48	22	22	15	1.19 ± 0.20	0.62 ± 0.27	0.09
6 week tail length	16	7	22	15	1.82 ± 0.30	0.40 ± 0.22	0.0002
10 week mass	53	22	21	11	1.07 ± 0.14	0.49 ± 0.21	0.03
10 week tail length	16	7	21	11	4.73 ± 0.36	0.86 ± 0.29	0.0001
Mandible length	39	20	21	10	2.19 ± 0.20	0.80 ± 0.27	0.0001
Mandible height	38	20	21	10	2.67 ± 0.21	0.77 ± 0.29	0.0001
Skull	39	20	13	5	1.94 ± 0.24	1.70 ± 0.44	0.63
Humerus	39	20	21	11	1.06 ± 0.21	0.78 ± 0.27	0.40
Ulna/radius	39	20	21	11	0.54 ± 0.19	0.66 ± 0.25	0.70
Femur	39	20	21	11	1.70 ± 0.22	0.85 ± 0.28	0.02
Tibia	39	20	21	11	1.11 ± 0.22	0.94 ± 0.28	0.63
Pelvic girdle	39	20	17	11	1.68 ± 0.23	1.13 ± 0.32	0.17

Values are in phenotypic standard deviation units for all traits, and are estimates (± standard error) of the differences between the least squares means of genotypes, from a model including the effects of experiment (i.e., osteoblast-specific or constitutive deletion), litter identity and sex.

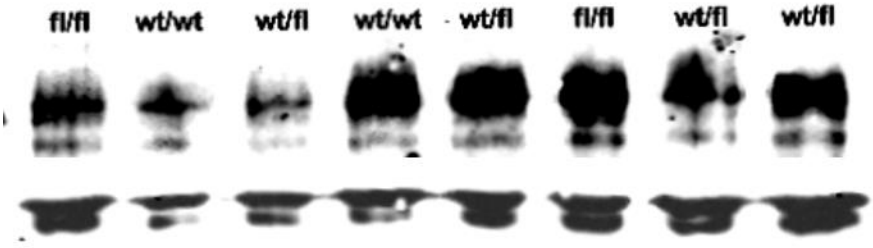

Figure 2.1. Effects of floxing on PAPP-A2 expression.
Western blot of PAPP-A2 in 8 placentae, homozygous for *Pappa2*^{fl} allele (fl/fl), heterozygotes (wt/fl), or homozygous for the wild-type *Pappa2*^{wt} allele (wt/wt). Top bands are PAPP-A2 protein and bottom bands are actin (internal control). The nitrocellulose membrane was scanned for fluorescence at 700 and 800 nm simultaneously, with fluorescence at 700 nm corresponding to actin (at approximately 40 kDa) and fluorescence at 800 nm corresponding to PAPP-A2 (at approximately 250 kDa).

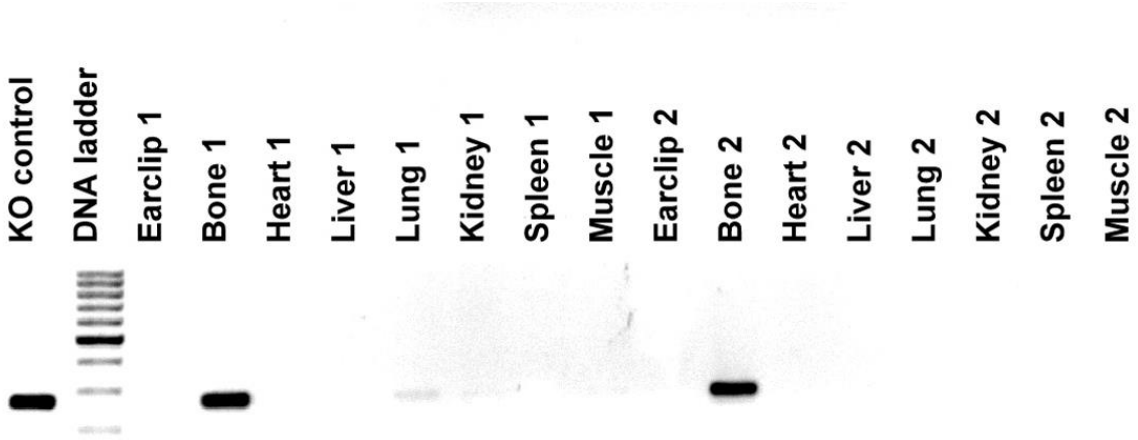

Figure 2.2. *Pappa2* deletion in bone.
PCR amplification of the *Pappa2* deletion allele (*Pappa2*^{KO}) in various tissues of two *Pappa2*$^{fl/fl}$;*Osx-Cre* mice (1 and 2). A positive control sample (earclip DNA from a homozygous constitutive deletion mouse) is in lane 1 and a 100 bp DNA ladder is in lane 2.

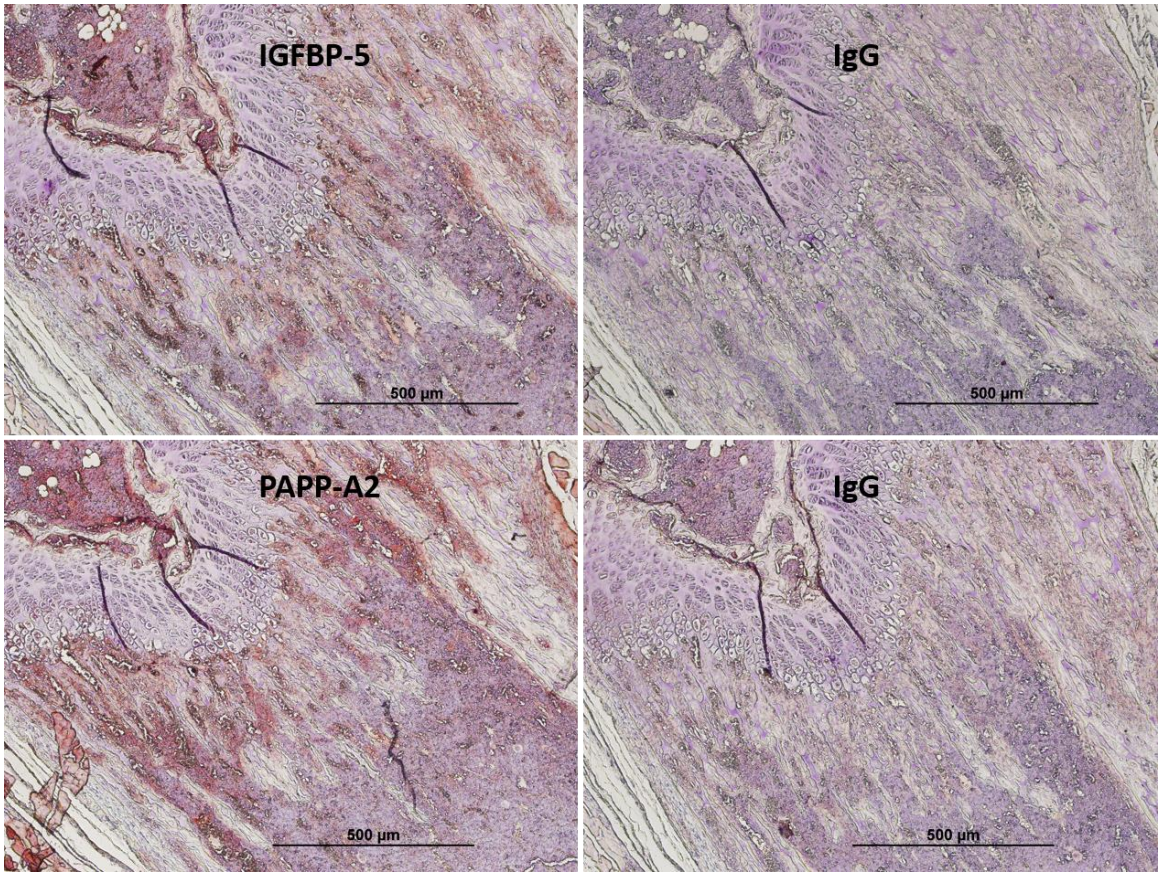

Figure 2.3. IGFBP-5 and PAPP-A2 localization in long bones.
Serial femoral sections stained for IGFBP-5 and PAPP-A2 and corresponding IgG control sections (right), all counterstained with hematoxylin and imaged at 10X magnification.

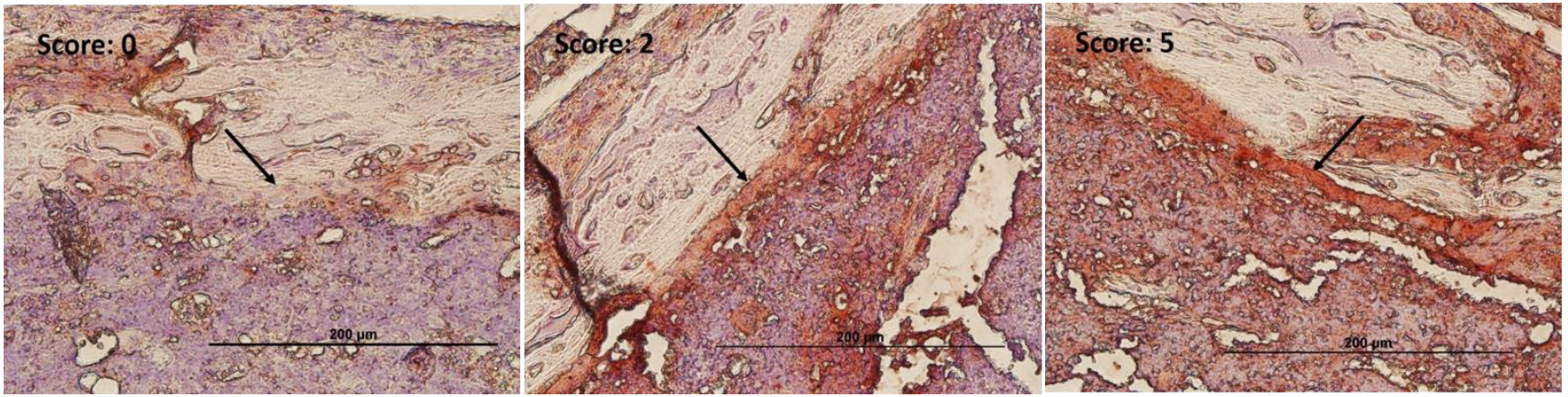

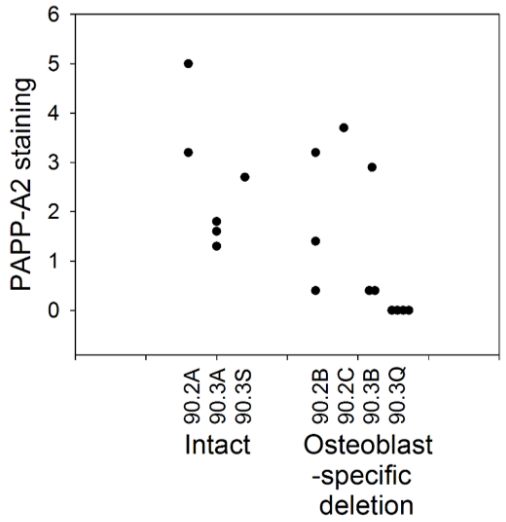

Figure 2.4. Blind-scoring of PAPP-A2 expression in osteoblasts.
Distribution of PAPP-A2 staining scores in osteoblasts of femurs from 3 control (intact) mice and 4 osteoblast-deletion mice. Each point represents the average score for one image from two individuals blind to genotype.

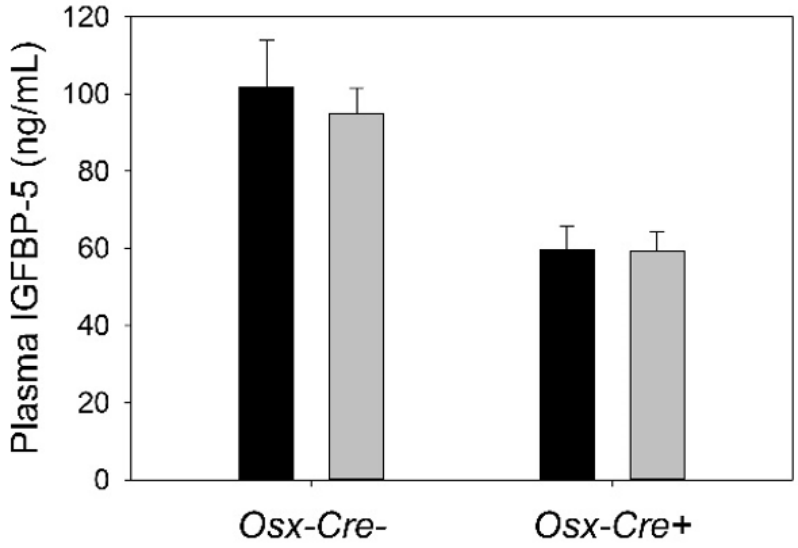

Figure 2.5. Effects of osteoblast-specific *Pappa2* deletion on plasma IGFBP-5 levels. Plasma IGFBP-5 in 18-19 day old mice homozygous (*Pappa2*$^{fl/fl}$; black bars) or heterozygous (*Pappa2*$^{wt/fl}$; grey bars) for the conditional *Pappa2* deletion allele and with or without the *Osx-Cre* transgene. Values are least square means (± standard error) from a model including effects of litter, *Pappa2* genotype, *Osx-Cre* genotype and the interaction between *Pappa2* and *Osx-Cre* genotype. *Osx-Cre*- was significantly different than *Osx-Cre*+.

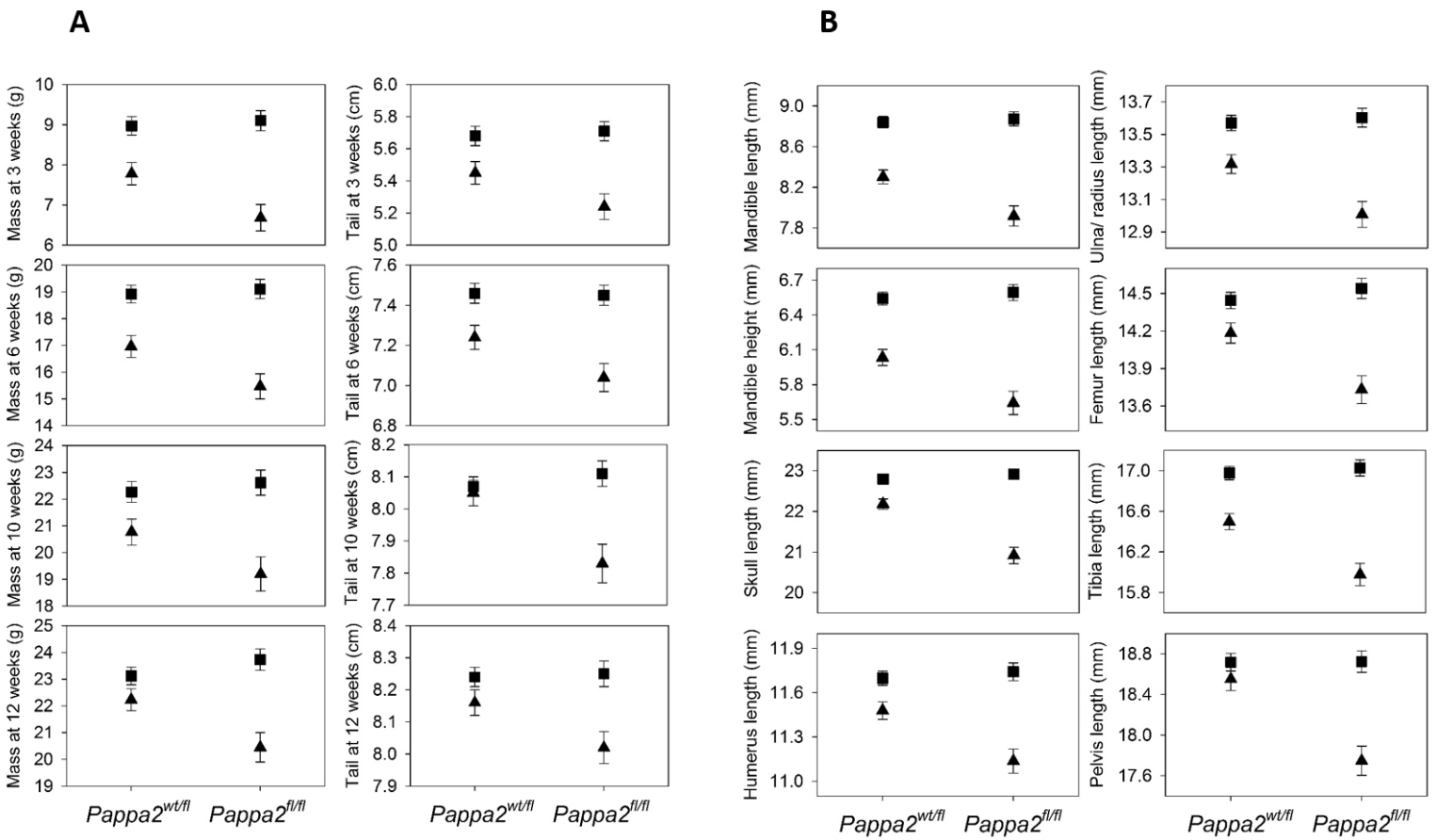

Figure 2.6. Effects of osteoblast-specific *Pappa2* deletion on post-natal growth.
Body mass and tail length at 3, 6, 10 and 12 weeks of age and bone dimensions at 12 weeks of age in mice heterozygous (*Pappa2*$^{wt/fl}$) and homozygous (*Pappa2*$^{fl/fl}$) for the conditional *Pappa2* deletion allele, with (triangle) or without (square) the *Osx-Cre* transgene. In all graphs, *Pappa2*$^{fl/fl}$ with Cre are significantly different than *Pappa2*$^{wt/fl}$ with Cre.

2.6. References

Atti E, Boskey A, Canalis E. 2005. Overexpression of IGF-binding protein 5 alters mineral and matrix properties in mouse femora: An infrared imaging study. Calcif Tissue Int 76:187-193.

Beattie J, Allan G, Lochrie J, Flint D. 2006. Insulin-like growth factor-binding protein-5 (IGFBP-5): A critical member of the IGF axis. Biochem J 395:1-19.

Bunn R, Fowlkes J. 2003. Insulin-like growth factor binding protein proteolysis. Trends in Endocrinology and Metabolism 14:176-181.

Chen J, Shi Y, Regan J, Karuppaiah K, Ornitz DM, Long F. 2014. Osx-cre targets multiple cell types besides osteoblast lineage in postnatal mice. Plos One 9:e85161.

Christians JK, Gruslin A. 2010. Altered levels of insulin-like growth factor binding protein proteases in preeclampsia and intrauterine growth restriction. Prenat Diagn 30:815-820.

Christians JK, Hoeflich A, Keightley PD. 2006. PAPPA2, an enzyme that cleaves an insulin-like growth-factor-binding protein, is a candidate gene for a quantitative trait locus affecting body size in mice. Genetics 173:1547-1553.

Christians JK, de Zwaan DR, Fung SHY. 2013. Pregnancy associated plasma protein A2 (PAPP-A2) affects bone size and shape and contributes to natural variation in postnatal growth in mice. Plos One 8:e56260.

Cohick WS, Clemmons DR. 1993. The insulin-like growth factors. Annu Rev Physiol 55:131-153.

Conover CA, Bale LK, Overgaard MT, Johnstone EW, Laursen UH, Fuchtbauer EM, Oxvig C, van Deursen J. 2004. Metalloproteinase pregnancy-associated plasma protein A is a critical growth regulatory factor during fetal development. Development 131:1187-1194.

Conover CA, Boldt HB, Bale LK, Clifton KB, Grell JA, Mader JR, Mason EJ, Powell DR. 2011. Pregnancy-associated plasma protein-A2 (PAPP-A2): Tissue expression and biological consequences of gene knockout in mice. Endocrinology 152:2837-2844.

Davey RA, Clarke MV, Sastra S, Skinner JP, Chiang C, Anderson PH, Zajac JD. 2012. Decreased body weight in young osterix-cre transgenic mice results in delayed cortical bone expansion and accrual. Transgenic Res 21:885-893.

Devlin RD, Du Z, Buccilli V, Jorgetti V, Canalis E. 2002. Transgenic mice overexpressing insulin-like growth factor binding protein-5 display transiently decreased osteoblastic function and osteopenia. Endocrinology 143:3955-3962.

Govoni K, Baylink D, Mohan S. 2005. The multi-functional role of insulin-like growth factor binding proteins in bone. Pediatr Nephrol 20:261-268.

Govoni KE, Lee SK, Chung Y, Behringer RR, Wergedal JE, Baylink DJ, Mohan S. 2007a. Disruption of insulin-like growth factor-I expression in type II alpha I collagen-expressing cells reduces bone length and width in mice. Physiological Genomics 30:354-362.

Govoni KE, Wergedal JE, Florin L, Angel P, Baylink DJ, Mohan S. 2007b. Conditional deletion of insulin-like growth factor-I in collagen type 1 alpha 2-expressing cells results in postnatal lethality and a dramatic reduction in bone accretion. Endocrinology 148:5706-5715.

Kaski JC, Holt DW. 2006. Pregnancy-associated plasma protein-A and cardiovascular risk. Eur Heart J 27:1637-1639.

Kjaer-Sorensen K, Engholm DH, Jepsen MR, Morch MG, Weyer K, Hefting LL, Skov LL, Laursen LS, Oxvig C. 2014. Pregnancy-associated plasma protein-A2 modulates development of cranial cartilage and angiogenesis in zebrafish embryos. J Cell Sci 127:5027-5037.

Miyakoshi N, Richman C, Kasukawa Y, Linkhart T, Baylink D, Mohan S. 2001. Evidence that IGF-binding protein-5 functions as a growth factor. J Clin Invest 107:73-81.

Mohan S, Baylink DJ. 2002. IGF-binding proteins are multifunctional and act via IGF-dependent and -independent mechanisms. J Endocrinol 175:19-31.

Mohan S, Richman C, Guo R, Amaar Y, Donahue L, Wergedal J, Baylink D. 2003. Insulin-like growth factor regulates peak bone mineral density in mice by both growth hormone-dependent and -independent mechanisms. Endocrinology 144:929-936.

Mukherjee A, Rotwein P. 2008. Insulin-like growth factor-binding protein-5 inhibits osteoblast differentiation and skeletal growth by blocking insulin-like growth factor actions. Molecular Endocrinology 22:1238-1250.

Overgaard MT, Boldt HB, Laursen LS, Sottrup-Jensen L, Conover CA, Oxvig C. 2001. Pregnancy-associated plasma protein-A2 (PAPP-A2), a novel insulin-like growth factor-binding protein-5 proteinase. J Biol Chem 276:21849-21853.

Parker EA, Hegde A, Buckley M, Barnes KM, Baron J, Nilsson O. 2007. Spatial and temporal regulation of GH-IGF-related gene expression in growth plate cartilage. J Endocrinol 194:31-40.

Phang D, Rehage M, Bonafede B, Hou D, Xing W, Mohan S, Wergedal JE, Qin X. 2010. Inactivation of insulin-like-growth factors diminished the anabolic effects of pregnancy-associated plasma protein-A (PAPP-A) on bone in mice. Growth Hormone & Igf Research 20:192-200.

Qin X, Wergedal JE, Rehage M, Tran K, Newton J, Lam P, Baylink DJ, Mohan S. 2006. Pregnancy-associated plasma protein-A increases osteoblast proliferation in vitro and bone formation in vivo. Endocrinology 147:5653-5661.

Rodda SJ, McMahon AP. 2006. Distinct roles for hedgehog and canonical wnt signaling in specification, differentiation and maintenance of osteoblast progenitors. Development 133:3231-3244.

Salih D, Mohan S, Kasukawa Y, Tripathi G, Lovett F, Anderson N, Carter E, Wergedal J, Baylink D, Pell J. 2005. Insulin-like growth factor-binding protein-5 induces a gender-related decrease in bone mineral density in transgenic mice. Endocrinology 146:931-940.

Salih D, Tripathi G, Holding C, Szestak T, Gonzalez M, Carter E, Cobb L, Eisemann J, Pell J. 2004. Insulin-like growth factor-binding protein 5 (Igfbp5) compromises survival, growth, muscle development, and fertility in mice. Proc Natl Acad Sci U S A 101:4314-4319.

Sheng MH-, Zhou X, Bonewald LF, Baylink DJ, Lau K-W. 2013. Disruption of the insulin-like growth factor-1 gene in osteocytes impairs developmental bone growth in mice. Bone 52:133-144.

Tanner SJ, Hefferan TE, Rosen CJ, Conover CA. 2008. Impact of pregnancy-associated plasma protein-A deletion on the adult murine skeleton. Journal of Bone and Mineral Research 23:655-662.

Wang J, Qiu Q, Haider M, Bell M, Gruslin A, Christians JK. 2009. Expression of pregnancy-associated plasma protein A2 during pregnancy in human and mouse. J Endocrinol 202:337-345.

Yakar S, Courtland H, Clemmons D. 2010. IGF-1 and bone: New discoveries from mouse models. Journal of Bone and Mineral Research 25:2267-2276.

Zhang W, Shen X, Wan C, Zhao Q, Zhang L, Zhou Q, Deng L. 2012. Effects of insulin and insulin-like growth factor 1 on osteoblast proliferation and differentiation: Differential signalling via akt and ERK. Cell Biochem Funct 30:297-302.

Chapter 3.

The role of PAPP-A2 in the acquisition and/or maintenance of bone mineral density in mice

3.1. Background

Osteoporosis impacts millions globally with affected individuals exhibiting low bone mass and micro-architectural deterioration of the skeleton (Rizzoli et al., 2001). Insulin like growth factors (IGFs) have been linked to the process of acquisition and maintenance of bone mineral density (BMD) as evident from human studies, bone cell culture experiments, and transgenic mice (Niu and Rosen, 2005; Rosen, 2004; Yakar et al., 2002). IGF-I is thought to be an important determinant of bone homeostasis and is involved in the formation and remodelling of bone through multiple stages of life (Giustina et al., 2008). The IGF system is involved in cellular proliferation, differentiation, and survival with IGF-I eliciting local and systemic actions (Cohick and Clemmons, 1993; Govoni et al., 2005; Mohan et al., 2003). Osteoblast-specific abolition of the type I IGF receptor (IGF-IR) resulted in a reduction of bone mineralization in mice (Zhang et al., 2002). Similarly, conditional deletion of IGF-I in the osteoblasts reduced bone formation (Govoni et al., 2007).

IGF-bioavailability is modulated by IGF binding proteins (IGFBPs), which act to prolong the half-lives of the IGFs and assist or inhibit their actions (Bunn and Fowlkes, 2003; Govoni et al., 2005; Mohan and Baylink, 2002; Salih et al., 2005). Of the binding proteins, IGFBP-5 is the most abundant in bone, working through IGF-dependent and independent pathways (Miyakoshi et al., 2001; Mohan and Baylink, 2002). Pregnancy associated plasma protein A and –A2 (PAPP-A and PAPP-A2) are paralog proteases: while PAPP-A cleaves both IGFBP-4 and -5, PAPP-A2 cleaves IGFBP-5, potentially regulating levels of intact IGFBP-5 (Overgaard et al., 2001) and consequently IGF actions in bone. *Pappa2* deletion mice exhibit inhibited postnatal growth (Conover et al., 2011), with bone lengths reduced more than would be expected given the reduction in body mass alone (Christians et al., 2013). However, the effects of PAPP-A2 on bone mineral density have yet to be studied. Because of the protease-substrate relationship, deletion of the *Pappa2* gene would be expected to increase levels of intact IGFBP-5. Previous mouse studies reveal paradoxical effects of increased IGFBP-5 on bone density (Mukherjee and Rotwein, 2007). Transgenic IGFBP-5 over-expression caused a decrease in BMD in two mouse

models (Atti et al., 2005; Devlin et al., 2002; Salih et al., 2005), and deletion of *Pappa*, which would be expected to increase IGFBP-5 levels, also lowered BMD (Tanner et al., 2008). By contrast, administration of recombinant IGFBP-5 to osteoblast cultures derived from IGF-I knockout mice and injection of IGFBP-5 to the same mice increased markers of bone formation (Miyakoshi et al., 2001) suggesting an increase in BMD. Additionally, administration of recombinant IGFBP-5 to ovariectomized mice, which are prone to lower BMD, increased BMD (Andress, 2001). These studies suggest opposing actions of IGFBP-5 in the bone depending on the initial physiological state of the model; i.e., increasing IGFBP-5 levels only increased bone density when bone formation was impaired/reduced at the onset of the study. However, other factors could also be contributing to these observations. Although these data indicate effects of IGFBP-5 on BMD, it is unclear whether PAPP-A2 is a sufficiently important regulator of bone IGFBP-5 to influence BMD. I predict that deleting *Pappa2* would act in a similar manner to increasing IGFBP-5 and thus reduce or increase BMD depending on the initial molecular and physiological state of the system, i.e., the state of pathways influenced by age in my models of study. To determine the role of PAPP-A2 in bone density, I sought to characterize bone phenotypes in mice with constitutive *Pappa2* deletion. Additionally, to eliminate the effects of body mass on BMD, I also examined a separate model with disruption of *Pappa2* in adulthood (Ruzankina et al., 2007). Lastly, I analyzed biomarkers of bone formation and bone resorption to determine whether the observed phenotypes were a consequence of changes in osteoblast and/or osteoclast lineages.

3.2. Methods

3.2.1. Ethics Statement

All work was carried out in accordance with the guidelines of the Canadian Council on Animal Care and approved by the SFU University Animal Care Committee (protocol 945B-09 and 1035B-11).

3.2.2. *Pappa2* deletion mice

Constitutive and conditional (adult) *Pappa2* deletion mice were generated as previously described (Christians et al., 2013). Mice heterozygous for the constitutive *Pappa2* disruption allele were paired to produce litters in which all three genotypes were present [i.e., homozygous

disruption (*Pappa2*$^{KO/KO}$), heterozygous (*Pappa2*$^{wt/KO}$), and homozygous wild-type (*Pappa2*$^{wt/wt}$)]. Phenotypes were characterized in at 12 weeks of age.

To produce adult-specific *Pappa2* deletion mice, mice with the conditional, floxed *Pappa2* allele (*Pappa2*$^{fl/fl}$) were bred to mice with tamoxifen-inducible *Cre* expression under the control of the human ubiquitin C promoter (*Ubc-Cre-ER*^{T2}) (Jackson Laboratory stock number 008085) (Ruzankina et al., 2007)). This cross generated *Pappa2*$^{fl/fl}$*Cre-ER*^{T2} mice and *Pappa2*$^{wt/wt}$ *Cre-ER*^{T2}control mice. Between 18 and 27 weeks of age (median age: 20 weeks), mice of both genotypes were injected once every 24 hours for five consecutive days with tamoxifen at a concentration of 75mg/kg body weight (Jackson Laboratory Tamoxifen Regimen, 2011). Despite treatment with tamoxifen, no *Pappa2* disruption is expected in the *Pappa2*$^{wt/wt}$ *Cre-ER*^{T2} mice due to the absence of "floxed" alleles. Males were euthanized 12-13 weeks after tamoxifen injection (i.e., 31-39 weeks of age, median age: 34 weeks). Adult-specific *Pappa2* deletion females were used as part of a separate breeding experiment and so were euthanized 31 weeks after tamoxifen injection (i.e., 49-55 weeks of age, median age: 50 weeks), at least 7 weeks after breeding. Adult specific individuals were much older than constitutive individuals due to the design of my studies; in order to eliminate body mass effects, adult specific *Pappa2* deletion mice were first allowed to reach full size and additional time was allocated for tamoxifen to take effect, resulting in a much older age compared to constitutive *Pappa2* deletion mice.

Constitutive *Pappa2* disruption was verified by PCR in a previous study (Christians et al., 2013). In the adult-specific study, removal of *Pappa2* exon 2 was assessed by PCR in the following tissues: earclip, lung, kidney, colon, ovaries, testes, prostate, and tibia (described below).

3.2.3. Genotyping

Mice were ear-clipped at three weeks of age and extraction of DNA was performed by standard methods. PCR genotyping was used for the determination of (a) *Pappa2* alleles, i.e., *Pappa2*^{wt}, *Pappa2*^{fl}, and *Pappa2*^{KO}, and (b) the presence/absence of the *Cre-ER*^{T2} transgene. Genotyping of *Pappa2* alleles used three primers designed to yield bands of different sizes for the three alleles (166 bp for *Pappa2*^{wt}, 305 bp for *Pappa2*^{fl} and 272 bp for *Pappa2*^{KO}). Primer sequences are as follows:

KO_prox (5'-CAGCAAAGGAAATTTGTGCT-3'),
KO_exon2 (5'-GGTCAAATGAAACTTCCCTCC-3'),
KO_dist2 (5'-CTC TTG CAT GCC TCC ACT AC-3').

The genotyping reactions for *Cre-ER*^{T2} included two primer pairs recommended by the Jackson Laboratory: one to amplify a fragment from the transgene and another to amplify a positive control fragment to confirm that the PCR was successful. The positive control primers target an exon of the *Interleukin 2* gene on chromosome 3. Primer sequences are as follows:

Cre_A (5'-GCGGTCTGGCAGTAAAAACTATC-3'),
Cre_B (5'-GTGAAACAGCATTGCTGTCACTT-3'),
Cre_+ve_A (5'-CTAGGCCACAGAATTGAAAGATCT-3'),
Cre_+ve_B (5'-GTAGGTGGAAATTCTAGCATCATCC-3').

3.2.4. Micro-computed tomography

Mice were sacrificed at 12 weeks (constitutive study), 34 weeks (adult-specific males) or 50 weeks (adult-specific females) and frozen at -20°C. These mice were thawed at a later date, the skin and internal organs were removed and the carcasses were dried to a constant weight before being exposed to dermestid beetles for removal of soft tissue. Femurs were obtained and scanned at the mid-diaphysis for cortical bone and distal metaphysis for trabecular bone. A total of 39 constitutive *Pappa2* deletion femurs comprising 20 males (7 *Pappa2*$^{wt/wt}$, 3 *Pappa2*$^{wt/KO}$, 10 *Pappa2*$^{KO/KO}$) and 19 females (6 *Pappa2*$^{wt/wt}$, 4 *Pappa2*$^{wt/KO}$, 9 *Pappa2*$^{KO/KO}$) were used. 24 adult-specific *Pappa2* deletion femurs consisting of 10 males (7 *Pappa2*$^{wt/wt}$*Cre-ER*^{T2}, 3 *Pappa2*$^{fl/fl}$*Cre-ER*^{T2}) and 14 females (6 *Pappa2*$^{wt/wt}$*Cre-ER*^{T2}, 8 *Pappa2*$^{fl/fl}$*Cre-ER*^{T2}) were examined.

Mouse femurs were scanned with micro-CT with an isotropic voxel size of 7.4µm (Scanco Medical µCT100, Bruttisellen, Switzarland; 70kVp, 114 µA, 100 ms integration time). All micro-CT scans were performed by a single trained operator at the Centre for High-Throughput Phenogenomics (University of British Columbia, Vancouver, Canada) and were analyzed according to the manufacturer's recommended protocol. Regions proportional to 5% of total length of bone were used to measure trabecular parameters in the distal metaphysis and cortical characteristics at the mid-shaft of each femur using morphological landmarks for standardization. For trabecular bone, the region of interest included just below the distal growth plate at the start of trabecular architecture and proceeded in the proximal direction, i.e., towards the middle of the

bone (the epiphysis and growth plate were not included in this process). The region of interest for cortical bone included the point from the disappearance of the third trochanter (where the cross-section of the bone transitions from a tear-drop shaped cortical ring to a round/oval shaped cortical ring), and continued for a number of slices proportional to the overall length of the bone in the distal direction. Standard morphological outcomes included: volumetric bone mineral density (BMD – bone density of total volume including cortical marrow) for the cortical and trabecular compartments separately (Tb. BMD and Ct. BMD), tissue mineral density (TMD – degree of mineralization of bone not including marrow), bone volume (BV mm^3) and total volume (TV mm^3); bone volume to total volume ratio (BV/TV – fraction of tissue volume to total volume not considering degree of mineralization), total cross-sectional area (TA, mm^2), bone area (BA), trabecular number (Tb.N,mm^{-1}), trabecular thickness (Tb.Th, mm), trabecular separation (Tb.Sp, mm), cortical thickness (Ct.Th, mm), volume of cortical medullary cavity (mm^3), and indices of resistance to force, including cross-sectional moment of inertia (Ixx and Imax – measures of bending/breaking strength) and the polar moment of inertia (pMOI – a measure of resistance to torsion). BV and TV refer to the volumes within the region of interest (ROI) and not the entire bone. Volume of the medullary cavity in the mid-shaft was calculated as the difference between TV and BV. Tb. BMD was calculated indirectly using algorithm provided by Scanco.

3.2.5. Serum PINP and TRACP 5b

To understand the underlying mechanisms influencing BMD changes, circulating levels of N-terminal propeptide of type I procollagen (PINP – a marker of bone formation) (AC-33F1 IDS Immunodiagnostics) and tartrate-resistant acid phosphatase form 5b (TRACP 5b – a marker of bone resorption) (SB-TR103 IDS Immunodiagnostics) were measured in constitutive *Pappa2* deletion females at 6 weeks (juvenile) and 19 weeks of age (adults). The immunoassays were performed in females for cost effectiveness and due to the availability of more female littermates with different genotypes.

3.3. Results

3.3.1. Analysis of body mass in the adult specific *Pappa2* deletion study

The least-squares means for body mass (g) were compared between *Pappa2*$^{wt/wt}$*Cre-ER*^{T2} and *Pappa2*$^{fl/fl}$*Cre-ER*^{T2} mice after cull. No genotypic effects were observed in the 24 individuals analyzed (data not shown).

3.3.2. *Pappa2* deletion after tamoxifen injection

Deletion of *Pappa2* was confirmed in tissues collected at cull from mice of both genders (2 males and 3 females). A representative image for one male and one female is provided below (Figure 3.1). In *Pappa2*$^{fl/fl}$*Cre-ER*^{T2} mice, PCR of DNA from the lung, kidney, colon, ovary, testes, the prostate, and tibia yielded both the deletion band and the floxed allele, indicating incomplete *Pappa2* deletion.

3.3.3. Effects of constitutive *Pappa2* deletion

Phenotypic effects of constitutive *Pappa2* deletion were determined by micro-computed tomography of femurs at trabecular and cortical regions from 12 week old individuals of both sexes. In a model containing litter, sex, and genotype, effects of *Pappa2* deletion were examined on several morphological parameters (Table 3.1). A sex*genotype interaction term was initially included but was not significant for any trait and so was removed. I compared the least squares means for each characteristic between wild-type (*Pappa2*$^{wt/wt}$), heterozygous for *Pappa2* deletion (*Pappa2*$^{wt/KO}$) and homozygous for *Pappa2* deletion *Pappa2*$^{KO/KO}$ mice (Table 3.1). Deletion of *Pappa2* resulted in overall increases in cortical BMD, BV/TV, and BA/TA (Table 3.1, Fig. 3.2). *Pappa2* deletion mice exhibited reduced values for volume (TV, BV) and cross-sectional area (TA, BA) (Table 3.1, Fig. 3.3), consistent with the reduced skeletal size demonstrated previously (Christians et al., 2013). While cortical thickness was not affected by *Pappa2* disruption, cortical medullary cavity volume was significantly smaller in *Pappa2*$^{KO/KO}$ individuals (Table 3.1). Additionally, values of Imax, pMOI, and Ixx were significantly lowered in the homozygous *Pappa2* deletion mice compared to control, suggesting changes bone strength (Table 3.1). In trabecular bone at the distal metaphysis, bone volume and trabecular thickness were reduced in the *Pappa2*$^{KO/KO}$ mice compared to the other genotypes (Table 3.1), however there was no change in BMD.

3.3.4. Effects of *Pappa2* deletion in adulthood

To assess the effects of *Pappa2* disruption independent of body mass effects, I compared bone characteristics in mice lacking PAPP-A2 after adult size was reached (*Pappa2*$^{fl/fl}$*Cre-ER*^{T2}) with those of control individuals (*Pappa2*$^{wt/wt}$*Cre-ER*^{T2}). Because of the large discrepancy in age between the sexes, the sexes were analysed separately. No genotypic effects were observed in the females. However, male *Pappa2* deletion mice exhibited decreased BV/TV and BMD (Figure 3.4) in addition to a lower bone volume (Table 3.2), despite no difference in total volume. Tb.N, and Tb.Sp were also reduced in *Pappa2*$^{fl/fl}$*Cre-ER*^{T2} individuals compared with controls (Table 3.2, Fig. 3.5).

3.3.5. Cellular consequences of constitutive *Pappa2* deletion in bone

To better understand the mechanism behind altered bone phenotypes observed in response to constitutive *Pappa2* deletion, I measured serum PINP (a bone formation marker of osteoblast activity) and TRACP 5b (bone resorption marker of osteoclast number) in 22 females at 6 weeks and 19 weeks of age. Levels of both PINP and TRACP 5b tended to be lower in knockout individuals at 6 weeks of age, although this was not significant (Table 3.3, Fig. 5.5). These patterns were also observed at 19 weeks of age, and PINP levels were significantly lower in knockout individuals ($\alpha = 0.05$) (Table 3.3, Fig. 3.5). Overall, levels of PINP decreased with age and levels of TRACP 5b increased with age.

3.4. Discussion

In this study, I sought to investigate the potential role(s) of PAPP-A2 in the acquisition and/or maintenance of bone mineral density in two mouse models with constitutive or adult-specific deletion of *Pappa2*. PAPP-A2 is a metalloproteinase targeting IGFBP-5, an inhibitory regulator of IGF-I with additional IGF-independent functions (Mohan and Baylink, 2002; Overgaard et al., 2001). In addition to examining the consequences of constitutive *Pappa2* disruption as described previously (Christians et al., 2013), I also studied potential effects of *Pappa2* deletion on a load-bearing bone independent of body mass by disrupting *Pappa2* after adulthood. Skeletal bones are comprised of varying degrees of cortical (compact) and trabecular (cancellous/spongy) bone (Clarke, 2008). I explored cortical properties in the mid-diaphysis of femora, while trabecular characteristics were determined in the distal metaphysis according to

guidelines suggested previously (Bouxsein et al., 2010). I demonstrate, for the first time, consequences of *Pappa2* disruption on the morphological properties of mouse femora using micro-computed tomography.

Constitutive disruption of *Pappa2* resulted in decreases in bone volume, cross-sectional area, and volume of the medullary cavity consistent with the decreased skeletal size as investigated previously (Christians et al., 2013). However, cortical bone mineral density (BMD), bone volume fraction (BV/TV), and fraction of cross-sectional area (BA/TA) were all increased in *Pappa2*$^{KO/KO}$ mice, indicating that *Pappa2* deletion affects not only size, but also bone accretion. The potentiating effects of *Pappa2* disruption on bone formation are consistent with mouse studies involving administration of recombinant IGFBP-5. Because PAPP-A2 targets IGFBP-5 (Overgaard et al., 2001), disruption of *Pappa2* could potentially be acting to increase levels of intact IGFBP-5. Andress (2001) observed a continuous increase in BMD in femurs and spine of ovariectomized mice in response to IGFBP-5 treatment (Andress, 2001). Similarly, administration of IGFBP-5 to mice with disruptions in the *Igf1* gene resulted in increases in levels bone formation markers and this finding was supported by in vitro IGFBP-5 treatment of bone cells (Miyakoshi et al., 2001). However, my findings are inconsistent with the decline in BMD in response to transgenic IGFBP-5 overexpression (Salih et al., 2004) and *Pappa* deletion (Tanner et al., 2008). The discrepancy between this study and previous studies may be due to variation in the initial physiological state of the model and mode of IGFBP-5 increase; these factors include age of the model, activity of age-dependent pathways in the model, system versus local changes in IGFBP-5, and the duration of IGFBP-5 increase. IGFBP-5 is thought to decrease levels of bioactive IGF-I, a bone promoting factor, therefore the increase in cortical BMD in response to *Pappa2* disruption hints at IGF-I independent actions of PAPP-A2 (an IGFBP-5 protease). Interestingly, cortical thickness remained constant across genotypes despite the changes in medullary cavity volume, indicating potential effects on bone strength. Values for indicators of strength, such as the cross-sectional moment of inertia (Ixx and Imax) as well as the polar moment of inertia (pMOI) were lower in the *Pappa2* deletion mice compared to heterozygotes and wildtype individuals, suggesting reductions in bone strength. However physical bending tests are necessary to validate these results.

Trabecular bone volume was significantly reduced in the constitutive *Pappa2* deletion mice consistent with the reduction in general skeletal size (Christians et al., 2013). Although I observed changes in the cortical bone mineral content, no changes in trabecular BMD were detected in

constitutive *Pappa2* deletion mice, suggesting a potentially differential and or diminished role of PAPP-A2 in trabecular bone. *Pappa2*$^{KO/KO}$ mice exhibited reductions in trabecular thickness, however, trabecular separation remained unchanged among genotypes. Although reductions in trabecular thickness may be indicative of bone loss or impaired bone formation, due to the lack in change in trabecular separation, it is likely that this was another by-product of reduced skeletal size.

My data suggest differential regulation of cortical and trabecular bone by PAPP-A2 in these mice. This is not surprising considering the dissimilarities in degree of mineralization, composition and structure, as well as mechanical properties between cortical and trabecular bone (Goodyear et al., 2009; Plowman and Smith, 2014). These differences underlie the distinct functions of cortical and trabecular bone; while cortical bone acts to provides structural support, trabecular bone acts to accommodate the physiological functions of the skeleton (Plowman and Smith, 2014). Moreover, cortical and trabecular bone display dissimilarities in the rate of bone turnover over an individual's lifespan and the degree of loss during different phases of aging (Alma Y. et al., 2013; Clarke, 2008; Zebaze et al., 2010). Additionally, diseases such as osteoporosis can affect cortical and trabecular bone to varying degrees and are thus classified based on this property (Shen et al., 2003). These factors combined may result in the differential regulation of cortical and trabecular bone by proteins such as PAPP-A2.

To determine a possible mechanism for the phenotypes observed in constitutive *Pappa2* deletion mice, I measured biomarkers of bone formation and bone resorption in females. Serum PINP was reduced in *Pappa2* deletion females compared to control littermates at both 6 (not significant) and 19 weeks (significant) of age, suggesting impaired osteoblast activity in these individuals. Levels of TRACP 5b were also reduced (not significantly) in *Pappa2* deletion females compared to control at both ages, suggesting decreases in osteoclast number. Decreases in both biomarkers suggests lower bone turn-over rates as early as 6 weeks of age in *Pappa2* deletion mice. Additionally, the data suggest that the increases in cortical BMD and BV/TV are more likely due to impaired bone resorption rather than potentiated bone formation. This is interesting as it suggests a potential role of PAPP-A2 in osteoclasts and/or pathways involving osteoclast action.

In examining effects of *Pappa2* deletion independent of body mass, disruption of the gene in adulthood had dissimilar effects compared to constitutive *Pappa2* deletion. Deletion of *Pappa2* in adulthood had no observable effects on cortical aspects of the femora. Additionally, the *Pappa2* deletion phenotype was evident in males alone, likely because the females were much older.

Adult male *Pappa2* deletion mice had reduced trabecular BMD and bone volume fraction (BV/TV), suggesting reductions in the amount of trabecular bone as well as the degree of mineralization compared to control individuals; a phenotype not observed in the constitutive deletion mice. Moreover, trabecular number was reduced while trabecular separation increased, suggesting a loss of trabecular architecture due to *Pappa2* disruption. However, my sample size is limited and these observations need to be further validated.

The combination of constitutive and adult-specific *Pappa2* deletion data suggest that PAPP-A2 is affecting bone physiology in a site-specific and age-specific manner in mice. The varying role of PAPP-A2 in different stages of life and type of bone may be due to variation in the initial physiological state of the system, i.e., differing IGFBP-5 and/or IGF-I levels. This highlights the complexity of the molecular pathways downstream of *Pappa2*; i.e., PAPP-A2 cleaves IGFBP-5, a binding protein shown to have IGF-dependent AND independent effects on bone physiology (Miyakoshi et al., 2001; Mohan and Baylink, 2002). Additionally, the variation in phenotypic consequences of increasing IGFBP-5 further contribute to the challenges in understanding regulation of the IGF system(Mukherjee and Rotwein, 2007). I predicted that PAPP-A2 deletion would influence bone mineral content. Consistent with my predictions, disruption of *Pappa2* led to changes in BMD and other morphological properties, however these phenotypes were age-specific and site-specific. Likely, reduced PAPP-A2 protein levels are increasing IGFBP-5 bioavailability and affecting both IGFBP-5 and IGF-I related processes in the bone.

3.5. Figures and Tables

Table 3.1 Effect of constitutive *Pappa2* deletion on bone.

Bone Parameters	*Pappa2*$^{wt/wt}$	*Pappa2*$^{wt/KO}$	*Pappa2*$^{KO/KO}$	P Value
Cortical Traits				
Total Volume (mm^3)	1.15 ± 0.02	1.15 ± 0.03	0.93 ± 0.02	<.0001*
Bone Volume (mm^3)	0.48 ± 0.01	0.47 ± 0.02	0.412 ± 0.009	<.0001*
BV/TV	0.420 ± 0.004	0.413 ± 0.005	0.442 ± 0.003	<.0001*
BMD (mg/cm^3)	394 ± 5	389 ± 7	427 ± 4	<.0001*
TMD(mg/cm^3)	1141 ± 6	1155 ± 8	1144 ± 5	0.447
Cortical Thickness (mm)	0.160 ± 0.002	0.159 ± 0.003	0.159 ± 0.002	0.959
Medullary Cavity (mm^3)	0.67 ± 0.01	0.67 ± 0.02	0.52 ± 0.01	<.0001*
Bone Area (mm^2)	0.67 ± 0.01	0.65 ± 0.02	0.58 ± 0.01	<.0001*
Total Area (mm^2)	1.58 ± 0.03	1.58 ± 0.04	1.31 ± 0.02	<.0001*
BA/TA	0.420 ± 0.004	0.413 ± 0.005	0.442 ± 0.003	<.0001*
pMOI (mm^4)	0.28 ± 0.01	0.27 ± 0.01	0.192 ± 0.009	<.0001*
Imax (mm^4)	0.183 ± 0.008	0.18 ± 0.01	0.123 ± 0.006	<.0001*
Ixx (mm^4)	0.14 ± 0.01	0.14 ± 0.01	0.098 ± 0.009	0.004*
Trabecular Traits				
Total Volume (mm^3)	1.39 ± 0.03	1.42 ± 0.04	1.17 ± 0.02	<.0001*
Bone Volume (mm^3)	0.121 ± 0.009	0.12 ± 0.01	0.102 ± 0.008	0.026*
BV/TV	0.082 ± 0.005	0.083 ± 0.007	0.083 ± 0.004	0.424
BMD (mg/cm^3)	75 ± 5	77 ± 7	76 ± 4	0.459
TMD(mg/cm^3)	909 ± 5	924 ± 7	916 ± 4	0.795
Trabecular Separation (mm)	0.219 ± 0.006	0.213 ± 0.009	0.209 ± 0.005	0.858
Trabecular Thickness (mm)	0.036 ± 0.0007	0.037 ± 0.001	0.034 ± 0.0006	0.016*
Trabecular Number (mm^{-1})	4.6 ± 0.1	4.7 ± 0.2	4.8 ± 0.1	0.798

Values are least square means (± standard error), from a model including sex and genotype. Sample sizes are as indicated in methods.

Table 3.2 Effects of adult-specific *Pappa2* deletion on bone.

Bone Parameters	Sex	*Pappa2*$^{wt/wt}$*Cre-ER*^{T2}	*Pappa2*$^{fl/fl}$*Cre-ER*^{T2}	P value
Cortical Traits				
Total Volume (mm³)	Male	1.70 ± 0.07	1.5 ± 0.1	0.232
	Female	1.34 ± 0.07	1.42 ± 0.06	0.421
Bone Volume (mm³)	Male	0.73 ± 0.02	0.64 ± 0.04	0.063
	Female	0.55 ± 0.03	0.627 ± 0.028	0.078
BV/TV	Male	0.44 ± 0.01	0.42 ± 0.02	0.518
	Female	0.41 ± 0.02	0.44 ± 0.02	0.241
BMD (mg/cm³)	Male	436 ± 17	409 ± 26	0.425
	Female	426 ± 29	482 ± 25	0.172
TMD(mg/cm³)	Male	1199 ± 7	1191 ± 11	0.545
	Female	1246 ± 10	1261 ± 9	0.307
Cortical Thickness (mm)	Male	0.188 ± 0.006	0.173 ± 0.010	0.248
	Female	0.167 ± 0.009	0.186 ± 0.008	0.131
Medullary Cavity (mm³)	Male	0.96 ± 0.06	0.88 ± 0.09	0.494
	Female	0.80 ± 0.06	0.79 ± 0.05	0.926
Bone Area (mm²)	Male	0.89 ± 0.03	0.78 ± 0.04	0.053
	Female	0.68 ± 0.04	0.77 ± 0.03	0.0998
Total Area (mm²)	Male	2.05 ± 0.08	1.9 ± 0.1	0.228
	Female	1.67 ± 0.09	1.74 ± 0.08	0.566
BA/TA	Male	0.44 ± 0.01	0.42 ± 0.02	0.518
	Female	0.41 ± 0.02	0.44 ± 0.02	0.241
pMOI (mm⁴)	Male	0.47 ± 0.03	0.38 ± 0.04	0.112
	Female	0.31 ± 0.02	0.33 ± 0.01	0.392
Imax (mm⁴)	Male	0.31 ± 0.02	0.25 ± 0.03	0.088
	Female	0.20 ± 0.01	0.201 ± 0.009	0.683
Ixx (mm⁴)	Male	0.23 ± 0.03	0.21 ± 0.05	0.751
	Female	0.14 ± 0.01	0.17 ± 0.01	0.086
Trabecular Traits				
Total Volume (mm³)	Male	1.6 ± 0.1	1.6 ± 0.2	0.957
	Female	1.45 ± 0.05	1.36 ± 0.04	0.175
Bone Volume (mm³)	Male	0.21 ± 0.02	0.11 ± 0.03	0.016*
	Female	0.020 ± 0.008	0.018 ± 0.007	0.874

BV/TV	Male	0.14 ± 0.02	0.07 ± 0.02	0.028*
	Female	0.014±0.006	0.014 ± 0.005	0.964
BMD (mg/cm^3)	Male	132 ± 15	62 ± 23	0.033*
	Female	15 ± 6	13 ± 5	0.905
TMD(mg/cm^3)	Male	959 ± 10	934 ± 16	0.224
	Female	962 ± 26	963 ± 23	0.975
Trabecular Separation (mm)	Male	0.245 ± 0.007	0.30 ± 0.01	0.002*
	Female	0.52 ± 0.03	0.49± 0.03	0.422
Trabecular Thickness (mm)	Male	0.046 ± 0.003	0.037 ± 0.004	0.079
	Female	0.032 ± 0.006	0.037 ± 0.005	0.541
Trabecular Number (mm-1)	Male	3.93 ± 0.09	3.2 ± 0.1	0.003*
	Female	2.00 ± 0.13	2.1 ± 0.1	0.665

Values are least square means (± standard error), from a model including a genotype by sex analysis. Sample sizes are as indicated in methods.

Table 3.3 Effect of constitute *Pappa2* deletion on PINP and TRACP 5b levels.

Bone Biomarker	Age	*Pappa2$^{fl/fl}$*	*Pappa2^{KOKO}*	P value
PINP (ng/mL)	6 weeks	375 ± 36	277 ± 36	0.0722
	19 weeks	30 ± 1	26 ± 1	0.0184*
TRACP 5b (U/L)	6 weeks	5.1 ± 0.4	4.1 ± 0.4	0.070
	19 weeks	13 ± 1	10 ± 1	0.100

Comparison of serum PINP and TRACP 5b levels between control (Pappa2flox) and constitutive knockout (Pappa2KO) females at 6 and 19 weeks of age. Values are least squares means ± standard error.

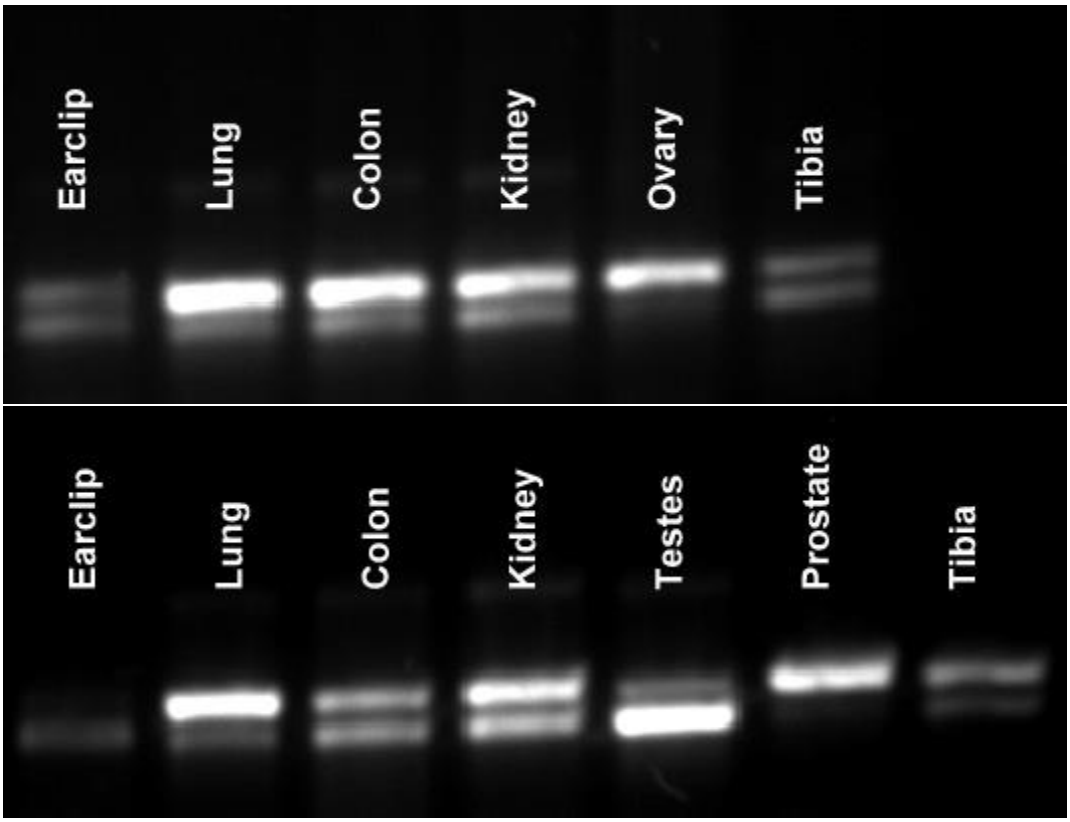

Figure 3.1. *Pappa2* deletion after tamoxifen injection.
Confirmation of partial disruption of the *Pappa2* gene after tamoxifen injection in tissue samples from *Pappa2*$^{fl/fl}$*Cre-ER*^{T2} individuals at cull using PCR; upper band indicates 305 bp flox [intact] allele and lower band indicates the 272 bp knockout allele. One representative image per sex; top image is female PCR, bottom image is male PCR.

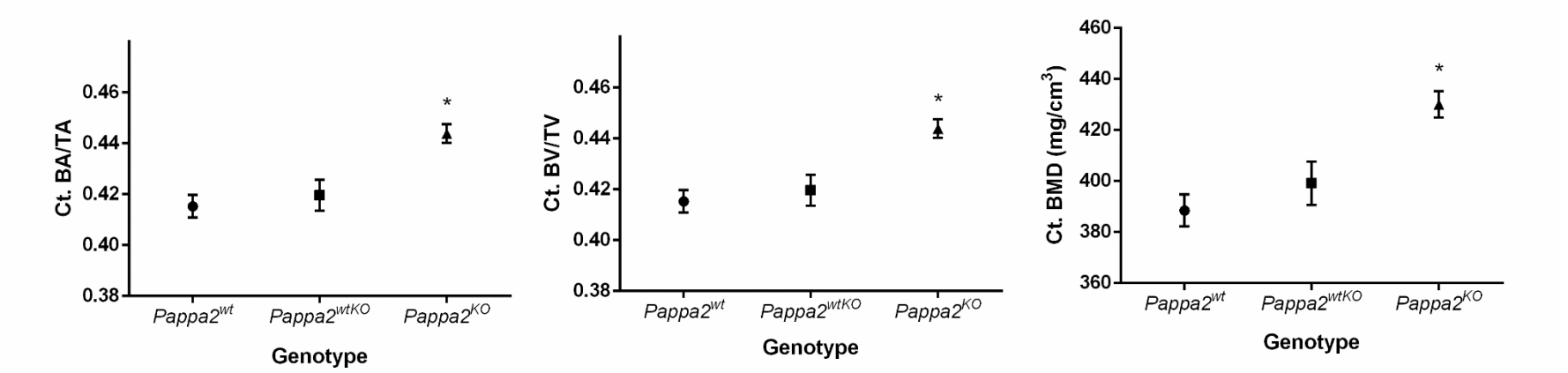

Figure 3.2. Constitutive *Pappa2* deletion effects on cortical bone formation.
Cortical cross-sectional areal fraction (Ct. BA/TA), bone volume fraction (Ct. BV/TV), and volumetric bone mineral density (Ct. BMD) in the constitutive *Pappa2* deletion study comparing *Pappa2*$^{wt/wt}$, *Pappa2*$^{wt/KO}$, and *Pappa2*$^{KO/KO}$ individuals of both sexes. Data is comparison of least mean squares (± standard error) in 39 individuals (details in methods). Asterisk denotes significance at α = 0.05.

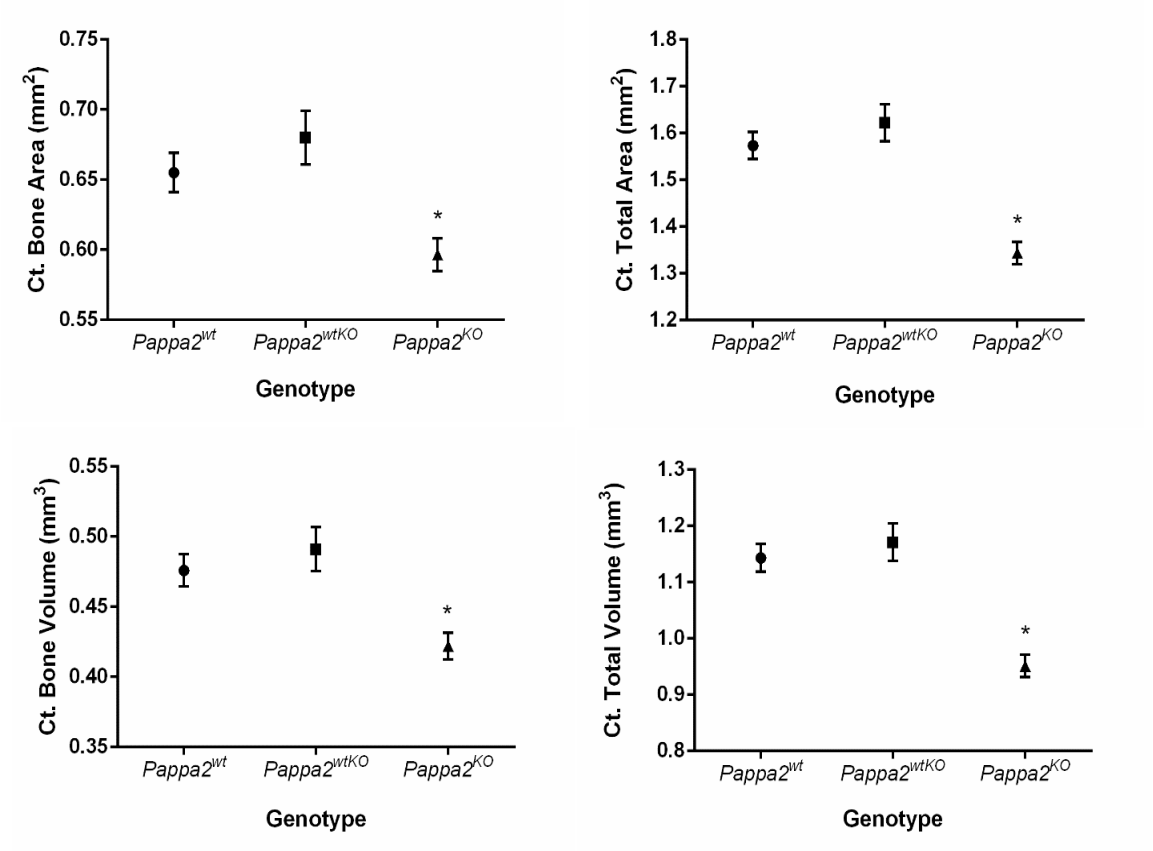

Figure 3.3. Consitutive *Pappa2* deletion effects on bone size.
Cortical bone area, total area of ROI, cortical bone volume, and total volume of ROI by genotype in the constitutive *Pappa2* deletion study. Least squares means (± standard error) plotted for *Pappa2*$^{wt/wt}$, *Pappa2*$^{wt/KO}$, and *Pappa2*$^{KO/KO}$ for both sexes. Asterisk denotes significance at α = 0.05.

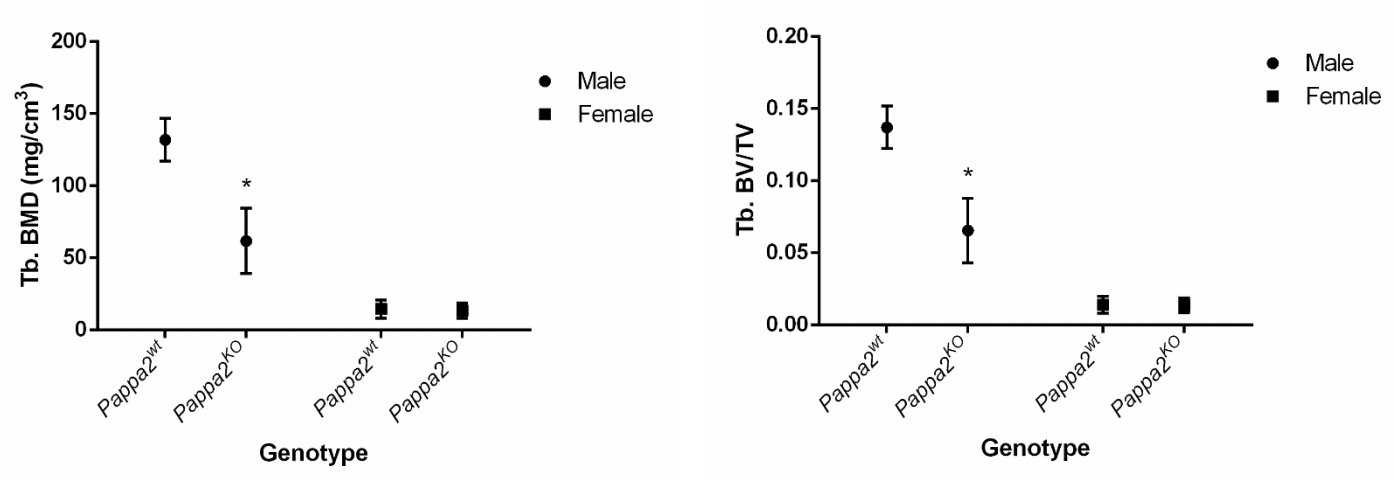

Figure 3.4. Effects of adult-specific *Pappa2* deletion on trabecular bone formation.
Trabecular bone mineral density (Tb. BMD) and bone volume fraction (Tb. BV/TV) compared by sex between *Pappa2*$^{wt/wt}$*Cre-ER*^{T2} (*Pappa2*$^{wt/wt}$) and *Pappa2*$^{fl/fl}$*Cre-ER*^{T2} (*Pappa2*$^{KO/KO}$). Least squares means (± standard error) plots of 10 males and 14 females (details in methods). Asterisk denotes significance at α = 0.05.

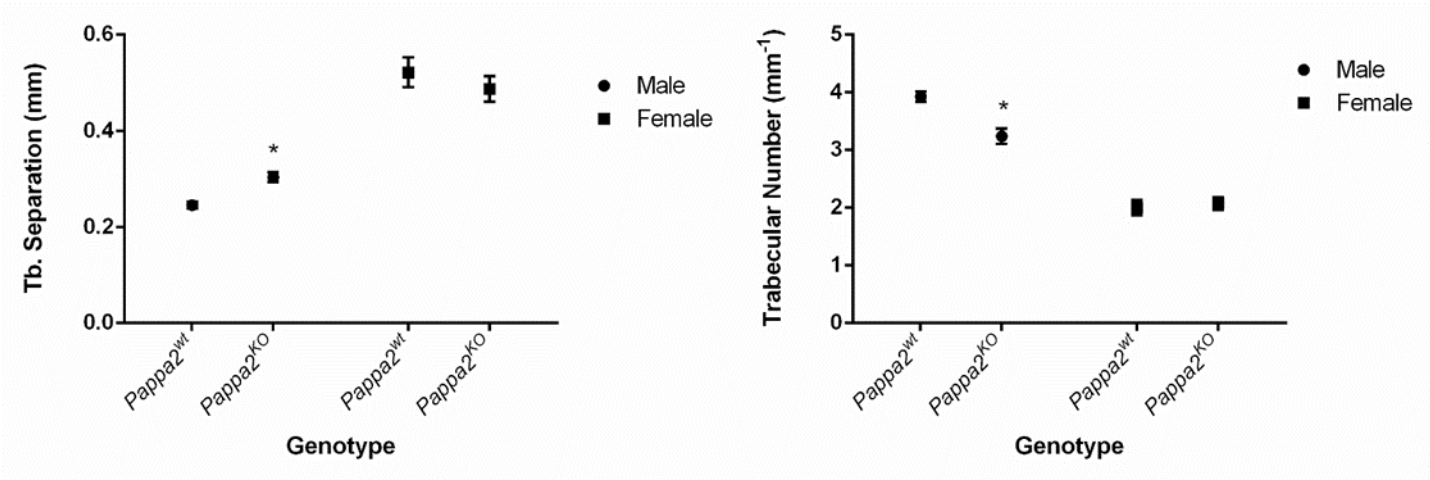

Figure 3.5. Effects of adult-specific *Pappa2* deletion on trabecular morphology.
Trabecular separation and thickness compared by sex between *Pappa2*$^{wt/wt}$*Cre-ER*^{T2} (*Pappa2*$^{wt/wt}$) and *Pappa2*$^{fl/fl}$*Cre-ER*^{T2} (*Pappa2*$^{KO/KO}$). Least squares means (± standard error) plots of 10 males and 14 females (details in methods). Asterisk denotes significance at α = 0.05.

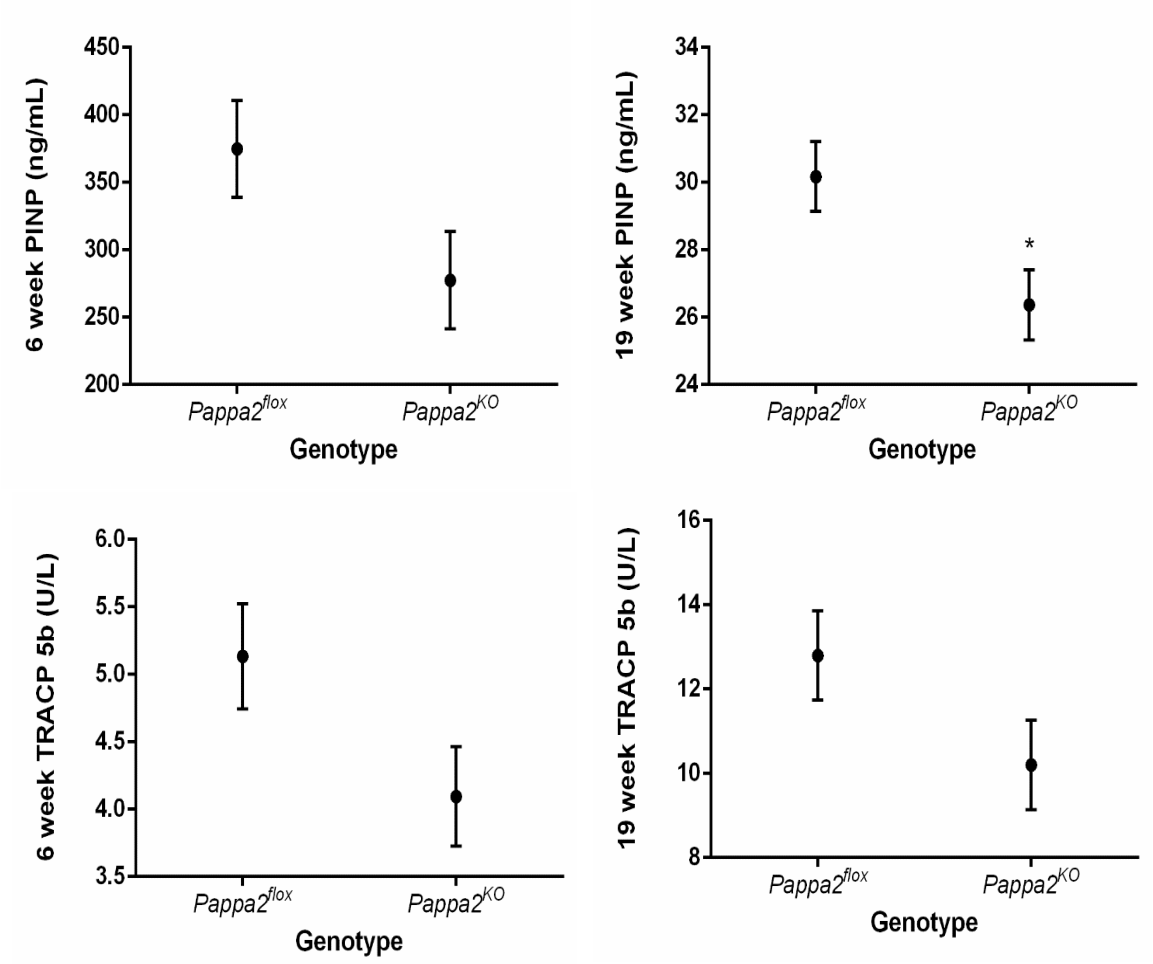

Figure 3.6. Serum chemistries in constitutive *Pappa2* deletion females.
Serum levels of PINP and TRACP 5b compared between constitutive *Pappa2* deletion (*Pappa2*$^{KO/KO}$) and control (*Pappa2*$^{fl/fl}$) females at 6 weeks and 19 weeks of age. Values are least squares means ± standard error. Asterisk denotes significance at α = 0.05.

3.6. References

Alma Y. P, Margarita V, Lorena O, Rafael V. Molecular aspects of bone remodeling.

Andress D. 2001. IGF-binding protein-5 stimulates osteoblast activity and bone accretion in ovariectomized mice. American Journal of Physiology-Endocrinology and Metabolism 281:E283-E288.

Atti E, Boskey A, Canalis E. 2005. Overexpression of IGF-binding protein 5 alters mineral and matrix properties in mouse femora: An infrared imaging study. Calcif Tissue Int 76:187-193.

Bouxsein ML, Boyd SK, Christiansen BA, Guldberg RE, Jepsen KJ, Mueller R. 2010. Guidelines for assessment of bone microstructure in rodents using micro-computed tomography. Journal of Bone and Mineral Research 25:1468-1486.

Bunn R, Fowlkes J. 2003. Insulin-like growth factor binding protein proteolysis. Trends in Endocrinology and Metabolism 14:176-181.

Christians JK, de Zwaan DR, Fung SHY. 2013. Pregnancy associated plasma protein A2 (PAPP-A2) affects bone size and shape and contributes to natural variation in postnatal growth in mice. Plos One 8:e56260.

Clarke B. 2008. Normal bone anatomy and physiology. Clin J Am Soc Nephrol 3 Suppl 3:S131-9.

Cohick WS, Clemmons DR. 1993. The insulin-like growth factors. Annu Rev Physiol 55:131-153.

Conover CA, Boldt HB, Bale LK, Clifton KB, Grell JA, Mader JR, Mason EJ, Powell DR. 2011. Pregnancy-associated plasma protein-A2 (PAPP-A2): Tissue expression and biological consequences of gene knockout in mice. Endocrinology 152:2837-2844.

Devlin RD, Du Z, Buccilli V, Jorgetti V, Canalis E. 2002. Transgenic mice overexpressing insulin-like growth factor binding protein-5 display transiently decreased osteoblastic function and osteopenia. Endocrinology 143:3955-3962.

Giustina A, Mazziotti G, Canalis E. 2008. Growth hormone, insulin-like growth factors, and the skeleton. Endocr Rev 29:535-559.

Goodyear SR, Gibson IR, Skakle JMS, Wells RPK, Aspden RM. 2009. A comparison of cortical and trabecular bone from C57 black 6 mice using raman spectroscopy. Bone 44:899-907.

Govoni K, Baylink D, Mohan S. 2005. The multi-functional role of insulin-like growth factor binding proteins in bone. Pediatr Nephrol 20:261-268.

Govoni KE, Wergedal JE, Florin L, Angel P, Baylink DJ, Mohan S. 2007. Conditional deletion of insulin-like growth factor-I in collagen type 1 alpha 2-expressing cells results in postnatal lethality and a dramatic reduction in bone accretion. Endocrinology 148:5706-5715.

Miyakoshi N, Richman C, Kasukawa Y, Linkhart T, Baylink D, Mohan S. 2001. Evidence that IGF-binding protein-5 functions as a growth factor. J Clin Invest 107:73-81.

Mohan S, Baylink DJ. 2002. IGF-binding proteins are multifunctional and act via IGF-dependent and -independent mechanisms. J Endocrinol 175:19-31.

Mohan S, Richman C, Guo R, Amaar Y, Donahue L, Wergedal J, Baylink D. 2003. Insulin-like growth factor regulates peak bone mineral density in mice by both growth hormone-dependent and -independent mechanisms. Endocrinology 144:929-936.

Mukherjee A, Rotwein P. 2007. Insulin-like growth factor binding protein-5 in osteogenesis: Facilitator or inhibitor? Growth Hormone & Igf Research 17:179-185.

Niu T, Rosen C. 2005. The insulin-like growth factor-I gene and osteoporosis: A critical appraisal. Gene 361:38-56.

Overgaard MT, Boldt HB, Laursen LS, Sottrup-Jensen L, Conover CA, Oxvig C. 2001. Pregnancy-associated plasma protein-A2 (PAPP-A2), a novel insulin-like growth factor-binding protein-5 proteinase. J Biol Chem 276:21849-21853.

Plowman SA, Smith DL. 2014. Exercise physiology for health, fitness, and performance. Philadelphia: Wolters Kluwer/Lippincott Williams & Wilkins Health. 734 p.

Rizzoli R, Bonjour J, Ferrari S. 2001. Osteoporosis, genetics and hormones. J Mol Endocrinol 26:79-94.

Rosen C. 2004. Insulin-like growth factor 1 and bone mineral density: Experience from animal models and human observational studies. Best Practice & Research Clinical Endocrinology & Metabolism 18:423-435.

Ruzankina Y, Pinzon-Guzman C, Asare A, Ong T, Pontano L, Cotsarelis G, Zediak VP, Velez M, Bhandoola A, Brown EJ. 2007. Deletion of the developmentallv essential gene ATR in adult mice leads to age-related phenotypes and stem cell loss. Cell Stem Cell 1:113-126.

Salih D, Kasukawa Y, Tripathi Q, Lovett F, Anderson N, Carter E, Wergedal J, Baylink J, Pell J, Mohan S. 2004. Transgenic overexpression of IGFBP-5 in mice leads to unexpected decrease in peak BMD in a gender specific manner: Evidence for IGF-independent mechanism of action. Journal of Bone and Mineral Research 19:S47-S47.

Salih D, Mohan S, Kasukawa Y, Tripathi G, Lovett F, Anderson N, Carter E, Wergedal J, Baylink D, Pell J. 2005. Insulin-like growth factor-binding protein-5 induces a gender-related decrease in bone mineral density in transgenic mice. Endocrinology 146:931-940.

Shen H, Recker RR, Deng HW. 2003. Molecular and genetic mechanisms of osteoporosis: Implication for treatment. Curr Mol Med 3:737-757.

Tanner SJ, Hefferan TE, Rosen CJ, Conover CA. 2008. Impact of pregnancy-associated plasma protein-A deletion on the adult murine skeleton. Journal of Bone and Mineral Research 23:655-662.

Yakar S, Rosen C, Beamer W *et al.* 2002. Circulating levels of IGF-1 directly regulate bone growth and density. J Clin Invest 110:771-781.

Zebaze RMD, Ghasem-Zadeh A, Bohte A, Iuliano-Burns S, Mirams M, Price RI, Mackie EJ, Seeman E. 2010. Intracortical remodelling and porosity in the distal radius and post-mortem femurs of women: A cross-sectional study. Lancet 375:1729-1736.

Zhang M, Xuan S, Bouxsein M *et al.* 2002. Osteoblast-specific knockout of the insulin-like growth factor (IGF) receptor gene reveals an essential role of IGF signaling in bone matrix mineralization. J Biol Chem 277:44005-44012.

Chapter 4.

Discussion and Conclusions

Pregnancy associated plasma protein A2 (PAPP-A2) is a serine metalloproteinase involved in the insulin-like growth factor (IGF) axis, targeting IGF binding protein 5 (IGFBP-5) (Overgaard et al., 2001). Since the initial discovery of PAPP-A2 as a paralog of pregnancy associated plasma protein A (PAPP-A) (Farr et al., 2000; Overgaard et al., 2001), PAPP-A2 has been the focus of very few studies. The IGF axis is a growth-promoting system with great complexity in organization and regulation; IGF-I acts through cell surface receptors in both a local and systemic fashion, while IGF binding proteins (IGFBPs) influence IGF bioavailability and biological action (Cohick and Clemmons, 1993; Mohan and Baylink, 2002). In bone, IGF-I affects cellular proliferation, differentiation and apoptosis, having a primarily stimulatory role (Govoni et al., 2005; Kasukawa et al., 2004). IGFBP-5 is the predominant binding protein in bone (Miyakoshi et al., 2001) acting to regulate IGF-I bioavailability and action (Mukherjee and Rotwein, 2008), while at the same time having IGF-independent effects (Beattie et al., 2006). Consequently, because PAPP-A2 decreases levels of intact IGFBP-5 (Overgaard et al., 2001), it is predicted to act on post-natal growth and bone physiology by increasing free IGF-I. Additionally, PAPP-A2 may also act on bone through IGF-independent pathways.

This thesis investigated the role of PAPP-A2 in post-natal growth and skeletal physiology through the use of three transgenic mouse lines to disrupt the *Pappa2* gene constitutively, spatially (in bone) or temporally (in adulthood). Given that *Pappa2* disruption has been shown to inhibit body growth and have a disproportionate effect on bone size (Christians et al., 2013; Conover et al., 2011), I predicted that deletion of bone-derived *Pappa2* would reduce bone growth. Additionally, I sought to examine effects of *Pappa2* disruption on bone mineral density in constitutive and adult-specific knockout models.

To understand the contribution of local versus systemic PAPP-A2, *Pappa2* was disrupted in bone using mice with expression of *Cre* recombinase under the control of the osteoblast-specific *Osterix* promoter (*Osx-Cre*) (Chapter 2). Disruption of *Pappa2* in bone reduces body mass and tail lengths at 3, 6, 10, and 12 weeks of age suggesting a role of

PAPP-A2 produced by bone in overall post-natal growth. Moreover, linear bone dimensions were also reduced implicating local PAPP-A2 in the regulation of longitudinal skeletal growth. Serum IGFBP-5 levels remained constant in bone-specific *Pappa2* deletion mice, suggesting the morphological effects were a result of changes to local PAPP-A2 action. Additionally, immunohistochemistry revealed co-localized expression of PAPP-A2 and IGFBP-5 in the epiphysis and metaphysis of long bones as well as osteoblasts. This is consistent with the hypothesis that local PAPP-A2 regulates IGFBP-5 protein and longitudinal bone growth. Interestingly, constitutive *Pappa2* deletion had greater effects than bone-specific *Pappa2* deletion for many traits, suggesting that postnatal growth is affected by PAPP-A2 produced by other tissues in addition to that produced by bone (Chapter 2).

Given evidence implicating IGFBP-5 in the regulation of bone density (Mukherjee and Rotwein, 2007), the role of PAPP-A2 in the maintenance of bone mineral density (BMD) and morphology was explored using micro-computed tomography (Chapter 3). In addition to studying constitutive *Pappa2* deletion effects on bone, an adult specific *Pappa2* disruption model was used to eliminate body mass effects on load-bearing bones. Analysis of femora revealed that constitutive *Pappa2* deletion increases cortical BMD, bone volume fraction (BV/TV), as well as cross sectional areal fraction (BA/TA) indicating anabolic consequences of PAPP-A2 deficiency. However, values for the cross-sectional moment of inertia (Ixx and Imax) and the polar moment of inertia (pMOI) were lower in the *Pappa2* deletion mice compared to heterozygotes and wildtype individuals, suggesting reductions in bone strength. This potential decrease in bone strength is likely due to *Pappa2* deletion bones having smaller diameters compared to the larger control bones, decreasing their physical strength properties; larger bones are stronger than smaller bones with similar BMD due to increased diameter (Clarke, 2008). However, measures of physical strength generated by micro-computed tomography have limitations and need to be validated through actual physical bending tests.

Although constitutive *Pappa2* deletion mice exhibit increased serum IGFBP-5 levels (Christians et al. 2014-unpublished), the increased BMD and bone volume fraction observed in *Pappa2* deletion mice are inconsistent with a molecular pathway involving increased intact IGFBP-5 protein and decreased IGF-I levels due to negative outcomes of

reduced IGF-I in BMD (Govoni et al., 2007; Sheng et al., 2013). More likely, the data suggest PAPP-A2 influences IGF-independent effects of IGFBP-5 in bone mineralization and growth. This prediction is supported by studies implicating IGFBP-5 in the regulation of post-natal growth, bone physiology, and bone mineral density (as covered in Chapters 2 & 3). Although no trabecular BMD effects were observed, constitutive *Pappa2* deletion mice exhibited reductions in trabecular thickness, likely because deletion bones were in general smaller. Increased cortical BMD and an absence of effect on trabecular bone mineral content suggests that PAPP-A2 may be more important for growth and development of cortical bone. Furthermore, there are substantial differences between structural properties, and the regulation and maintenance of these properties in cortical and trabecular bone within individuals and between sexes (Clarke, 2008; Seeman et al., 1982; Shahnazari et al., 2011). Cortical bone accounts for 75-80% of bone, however, trabecular bone has a 10 fold higher rate of bone turnover and a higher turnover rate compared to cortical bone (Alma Y. et al., 2013; Clarke, 2008). While both cortical and trabecular bone undergo age-related deterioration, a cross-sectional study demonstrated that the initial rapid loss of bone following menopause is trabecular. However, after the age of 65, cortical bone contributes to the majority of bone loss, comprising up to 90% of bone loss by 80 years of age (Zebaze et al., 2010). The differential degree of bone loss demonstrates potential molecular and/or physiological differences between cortical and trabecular bone. PAPP-A2 may be one pathway acting differentially in cortical and trabecular bone.

To understand the mechanisms behind increased BMD in response to constitutive *Pappa2* disruption, serum contents of PINP (a bone formation marker) and TRACP 5b (a bone resorption marker) were analyzed in 6 and 19 week females. PINP and TRACP 5b demonstrated decreased trends in *Pappa2* deletion mice at both ages, suggesting reduced bone turnover. Additionally, because TRACP 5b was lower in *Pappa2* deletion mice, but PINP was not higher, it can be predicted that the increase in BMD as observed in this model is more likely due to inhibited osteoclast-mediated resorption rather than increased osteoblast-induced bone apposition. If true, this prediction could implicate PAPP-A2 in pathways involving osteoclast cells in bone. The Notch signalling pathways present in both cell types (Regan and Long, 2013) and has been demonstrated to potentially be regulated by PAPP-A2 in zebrafish embryos (Kjaer-Sorensen et al., 2014).

Adult-specific *Pappa2* deletion mice did not exhibit any changes to cortical bone morphology or strength, suggesting that PAPP-A2 has a diminished role in cortical compartments during adulthood compared to previous stages of life. Disruption of *Pappa2* in adulthood decreased trabecular BMD and bone volume fraction in males. Moreover, trabecular number decreased in *Pappa2* disruption males while trabecular separation increased, suggesting the loss of trabecular connections due to *Pappa2* deletion. The differential phenotypic effects of *Pappa2* disruption on cortical vs. trabecular bone morphology in adult mice further suggests potential site-specific roles of PAPP-A2 in bone. In humans, both serum and skeletal levels of IGFBP-5 and IGF-I have been shown to significantly decrease with age and are thought to be independent changes, i.e., decreases of IGF components in bone are not a direct result of decreases in serum levels (Mohan et al., 1995). PAPP-A2 may be regulating bone differentially depending on the biological levels of IGFBP-5 and IGF-I.

This thesis suggests that PAPP-A2 functions not only in post-natal growth and longitudinal skeletal growth (Chapter 2), but also in the acquisition and maintenance of bone density (Chapter 3). The mode of PAPP-A2 action still remains to be investigated and it is unclear whether the observed effects are related to changes in IGFBP-5 and/or IGF-I bioactivity. However, it is feasible that some PAPP-A2 action relates to its biological function of regulating IGFBP-5 availability. In mice, deletion of IGF-I in bone has growth-inhibiting consequences (Govoni et al., 2007; Govoni et al., 2008; Sheng et al., 2013) similar to the bone-specific *Pappa2* deletion phenotypes, suggesting some parallels between decreases in local levels of PAPP-A2 and IGF-I. However, contrary to the constitutive knockouts, disruption of *Igf1* has been shown to negatively affect the acquisition/maintenance of BMD (Govoni et al., 2007; Govoni et al., 2008; Sheng et al., 2013). The phenotypic consequences of increased IGFBP-5 levels in mice on BMD are context-dependent, showing both potentiating and inhibiting roles depending on the system (Mukherjee and Rotwein, 2007). This suggests that PAPP-A2 could potentially be regulating BMD in a similar fashion, i.e., exerting positive or negative effects depending on other physiological factors. This prediction is consistent with my data, as I observed increases in cortical BMD in the constitutive *Pappa2* deletion mice, yet no difference in the same site in the adult-specific mice. Interestingly, a recent study in zebrafish suggests a potential role of PAPP-A2 outside the IGF axis involving regulation of Notch signalling in

embryonic development (Kjaer-Sorensen et al., 2014). In both humans and mice, Notch signalling is important for skeletal development, the remodelling of bone, and regulation of BMD, acting in bone osteoblasts and osteoclast pathways (Regan and Long, 2013).

Although my findings shed light on the possible functions of PAPP-A2, they raise even more questions regarding the molecular pathways of PAPP-A2 action in skeletal growth and bone health. The plausible pathways include IGF-dependent and/or independent actions of IGFBP-5, and IGFBP-5 independent mechanisms. It is important that future studies delve more specifically into the molecular mechanisms of PAPP-A2 action, including investigating other possible targets for PAPP-A2 action. Potential mechanisms could include osteoclast-related pathways and Notch signalling.

Osteoporosis, a skeletal disorder entailing the loss of bone mass and alterations of bone microarchitecture (Rizzoli et al., 2001), is expected to rise in incidence due to an aging population (Gullberg et al., 1997). Although no definitive cure exists for the disease, IGF-I has received substantial attention due to association with bone development and maintenance (Kasukawa et al., 2004). However, because of the comprehensive and extensive actions of IGF-I reaching a multitude of tissue types, future research must explore molecular regulators of IGF-I as potential therapeutic targets to bypass potential adverse effects with its chronic use. This thesis shows that PAPP-A2 contributes to the regulation of skeletal growth and bone mineralization in mice.

4.1. References

Alma Y. P, Margarita V, Lorena O, Rafael V. 2013. Molecular aspects of bone remodeling.

Beattie J, Allan G, Lochrie J, Flint D. 2006. Insulin-like growth factor-binding protein-5 (IGFBP-5): A critical member of the IGF axis. Biochem J 395:1-19.

Christians JK, de Zwaan DR, Fung SHY. 2013. Pregnancy associated plasma protein A2 (PAPP-A2) affects bone size and shape and contributes to natural variation in postnatal growth in mice. Plos One 8:e56260.

Clarke B. 2008. Normal bone anatomy and physiology. Clin J Am Soc Nephrol 3 Suppl 3:S131-9.

Cohick WS, Clemmons DR. 1993. The insulin-like growth factors. Annu Rev Physiol 55:131-153.

Conover CA, Boldt HB, Bale LK, Clifton KB, Grell JA, Mader JR, Mason EJ, Powell DR. 2011. Pregnancy-associated plasma protein-A2 (PAPP-A2): Tissue expression and biological consequences of gene knockout in mice. Endocrinology 152:2837-2844.

Farr M, Strube J, Geppert H, Kocourek A, Mahne M, Tschesche H. 2000. Pregnancy-associated plasma protein-E (PAPP-E). Biochimica Et Biophysica Acta-Gene Structure and Expression 1493:356-362.

Govoni K, Baylink D, Mohan S. 2005. The multi-functional role of insulin-like growth factor binding proteins in bone. Pediatr Nephrol 20:261-268.

Govoni KE, Lee SK, Chung Y, Behringer RR, Wergedal JE, Baylink DJ, Mohan S. 2007. Disruption of insulin-like growth factor-I expression in type II alpha I collagen-expressing cells reduces bone length and width in mice. Physiological Genomics 30:354-362.

Govoni KE, Wergedal JE, Chadwick RB, Srivastava AK, Mohan S. 2008. Prepubertal OVX increases IGF-I expression and bone accretion in C57BL/6J mice. American Journal of Physiology-Endocrinology and Metabolism 295:E1172-E1180.

Govoni KE, Wergedal JE, Florin L, Angel P, Baylink DJ, Mohan S. 2007. Conditional deletion of insulin-like growth factor-I in collagen type 1 alpha 2-expressing cells results in postnatal lethality and a dramatic reduction in bone accretion. Endocrinology 148:5706-5715.

Gullberg B, Johnell O, Kanis JA. 1997. World-wide projections for hip fracture. Osteoporosis Int 7:407-413.

Kasukawa Y, Miyakoshi N, Mohan S. 2004. The anabolic effects of GH/IGF system on bone. Curr Pharm Des 10:2577-2592.

Kjaer-Sorensen K, Engholm DH, Jepsen MR, Morch MG, Weyer K, Hefting LL, Skov LL, Laursen LS, Oxvig C. 2014. Pregnancy-associated plasma protein-A2 modulates development of cranial cartilage and angiogenesis in zebrafish embryos. J Cell Sci 127:5027-5037.

Miyakoshi N, Richman C, Kasukawa Y, Linkhart T, Baylink D, Mohan S. 2001. Evidence that IGF-binding protein-5 functions as a growth factor. J Clin Invest 107:73-81.

Mohan S, Baylink DJ. 2002. IGF-binding proteins are multifunctional and act via IGF-dependent and -independent mechanisms. J Endocrinol 175:19-31.

Mohan S, Farley JR, Baylink DJ. 1995. Age-related changes in IGFBP-4 and IGFBP-5 levels in human serum and bone: Implications for bone loss with aging. Prog Growth Factor Res 6:465-473.

Mukherjee A, Rotwein P. 2008. Insulin-like growth factor-binding protein-5 inhibits osteoblast differentiation and skeletal growth by blocking insulin-like growth factor actions. Molecular Endocrinology 22:1238-1250.

Mukherjee A, Rotwein P. 2007. Insulin-like growth factor binding protein-5 in osteogenesis: Facilitator or inhibitor? Growth Hormone & Igf Research 17:179-185.

Overgaard MT, Boldt HB, Laursen LS, Sottrup-Jensen L, Conover CA, Oxvig C. 2001. Pregnancy-associated plasma protein-A2 (PAPP-A2), a novel insulin-like growth factor-binding protein-5 proteinase. J Biol Chem 276:21849-21853.

Regan J, Long F. 2013. Notch signaling and bone remodeling. Current Osteoporosis Reports 11:126-129.

Rizzoli R, Bonjour J, Ferrari S. 2001. Osteoporosis, genetics and hormones. J Mol Endocrinol 26:79-94.

Seeman E, Wahner H, Offord K, Kumar R, Johnson W, RIGGS B. 1982. Differential-effects of endocrine dysfunction on the axial and the appendicular skeleton. J Clin Invest 69:1302-1309.

Shahnazari M, Yao W, Wang B, Panganiban B, Ritchie RO, Hagar Y, Lane NE. 2011. Differential maintenance of cortical and cancellous bone strength following discontinuation of bone-active agents. Journal of Bone and Mineral Research 26:569-581.

Sheng MH-, Zhou X, Bonewald LF, Baylink DJ, Lau K-W. 2013. Disruption of the insulin-like growth factor-1 gene in osteocytes impairs developmental bone growth in mice. Bone 52:133-144.

Zebaze RMD, Ghasem-Zadeh A, Bohte A, Iuliano-Burns S, Mirams M, Price RI, Mackie EJ, Seeman E. 2010. Intracortical remodelling and porosity in the distal radius and post-mortem femurs of women: A cross-sectional study. Lancet 375:1729-1736.